# The cryptic stratigraphic record of the syn- to post-rift transition in the offshore Campos Basin, SE Brazil

Francyne Bochi do Amarante[1,#]

[1] Instituto de Geociências, Universidade Federal do Rio Grande do Sul, Porto Alegre, 90650 001, Brazil

[#] corresponding author francyne.amarante@ufrgs.br

ORCID https://orcid.org/0000-0003-4452-8635

Juliano Kuchle[1]

[1] Instituto de Geociências, Universidade Federal do Rio Grande do Sul, Porto Alegre, 90650 001, Brazil

juliano.kuchle@ufrgs.br

ORCID https://orcid.org/0000-0003-4325-0547

Christopher Aiden-Lee Jackson[2,3]

[2] Jacobs, Manchester, M15 4GU, United Kingdom

[3] Basins Research Group (BRG), Department of Earth Science and Engineering, Imperial College London, London, SW7 2BP, United Kingdom

christopher.jackson@manchester.ac.uk

ORCID https://orcid.org/0000-0002-8592-9032

Claiton Marlon dos Santos Scherer[1]

[1] Instituto de Geociências, Universidade Federal do Rio Grande do Sul, Porto Alegre, 90650 001, Brazil

claiton.scherer@ufrgs.br

ORCID https://orcid.org/0000-0002-7520-1187

Leonardo Muniz Pichel[4]

[3] Department of Earth Science, University of Bergen, 5007, Bergen, Norway

leonardo.m.pichel@uib.no

ORCID https://orcid.org/0000-0001-8692-3831

**This manuscript is a preprint** and has been submitted for publication in **Basin Research**. Please note that this manuscript has not yet undergone peer-review; as such, subsequent version of this manuscript may have different content. We invite you to contact any of the authors directly to comment and give any feedbacks on the manuscripts.

## Abstract

Rift basins typically comprise three main tectono-stratigraphic stages; pre-, syn-, and post-rift. The syn-rift stage is often characterised by the deposition of asymmetric wedges of growth strata that record differential subsidence caused by active normal faulting. The subsequent post-rift stage is defined by long-wavelength subsidence driven by lithospheric cooling, and is typified by the deposition of broadly tabular stratal packages that drape any rift-related relief. The stratigraphic contact between syn- and post-rift rocks is often thought to be represented by an erosional unconformity. However, the late syn-rift to early post-rift stratigraphic record is commonly far more complex since: (i) the associated tectonic transition is not instantaneous; (ii) net-subsidence may be punctuated by transient periods of uplift; and (iii) strain often migrates oceanward during rifting until continental breakup is achieved with crustal rupture. The Eastern Brazilian marginal basins have not historically used the tripartite scheme outlined above, with the post-pre-rift interval instead being subdivided into rift, sag, and passive margin tectono-stratigraphic stages. The sag stage has been previously described as late syn-rift, early post-rift, or as a transition between the two, with the passive margin stage being equivalent to the classically defined post-rift, drift stage. Two (rather than one) erosional unconformities are also identified within the rift-to-sag succession. In this work, we use 2D and 3D seismic reflection and borehole data to discuss the expression of and controls on the syn- to post-rift transition in the shallow and deep water domains of the south-central Campos Basin, southeast Brazil. We identified three seismic-stratigraphic sequences bounded by unconformities. The lower pre-salt interval is characterised by wedge-shaped packages of reflections that thicken towards graben and half-graben-bounding normal faults. This stage ends with a development of an angular unconformity, inferred to form as a result of the onset of the oceanward migration of deformation. The

upper pre-salt is typically defined by packages of subparallel and relatively continuous reflections that are broadly lenticular and thin towards fault-bound basement highs, but that locally contain packages that thicken against faults. The pre-salt to salt contact is defined by an erosional unconformity that is largely restricted to basement highs, and which is inferred to have formed due to base-level fall and uplift associated with local fault reactivation, resulting in the formation of channels of possible fluvial origin. Based on its geometries and seismic facies, we conclude that the lower pre-salt interval is syn-rifting and *syn-tectonic*, deposited during active continental extension and upper crustal faulting affecting the entire evolving margin, whereas the overlying upper pre-salt is syn-rifting and *post-tectonic* in the Campos Basin, deposited when extension and faulting had migrated seaward to the future location of the spreading centre. The results of our study support the arising notion that the syn-rift sequence does not only displays syn-tectonic sedimentary packages, and thus the tripartite tectono-stratigraphic model for rift development is too simplistic and cannot be applied when assessing rifts in the context of the regional development of continental margins.

*Keywords*: pre-salt reservoirs, sag basin, rift basin, South Atlantic basins, continental margins, unconformity.

## 1. Introduction

The tectonic evolution of rift basins comprise three main tectono-stratigraphic stages: pre-, syn-, and post-rift. Classical models of rift basin evolution are based on the analysis of the sedimentary record preserved within individual grabens and half-grabens; studies such as these typically allow the timing and duration of these stages to be constrained (e.g. Prosser, 1993; Bosence, 1998; Gawthorpe and Leeder, 2000). In these

models, the syn-rift stage is characterised by mechanical subsidence, marked by the generation of large amounts of accommodation over a relatively short period. Mechanical subsidence occurs due to movement/slip along normal faults and the associated rotation of intervening fault blocks, resulting in differential subsidence and the formation of grabens or half-grabens, separated by horsts (i.e. basement highs). During this time (named *mid syn-rift* by Bosence, 1998, and *rift climax* by Prosser, 1993 and Kuchle and Scherer, 2010), the greatest thickness of sediment accumulates next to the half-graben border fault; in the case of a symmetrical graben, sediment thicken across the bounding faults, into the intervening depocentre. Following the main *syn-rift* period or *rift climax*, active faulting gradually decreases and ceases (Gawthorpe and Leeder, 2000), and mechanical subsidence is replaced by a long-wavelength, relatively slow subsidence driven by cooling of the lithosphere (Prosser, 1993; Bosence, 1998). In some cases, this transition is associated with plate rupture (i.e. plate breakup) and the steady-state emplacement of oceanic crust. Plate rupture and oceanic spreading lead to greater thermal subsidence by cooling of the newly formed magmatic crust and exhumed mantle (and thus, increasing the density), and the formation of a rifted margin (see below; see also Bott, 1995). When rupture does not occur, rifting is considered to have failed (Allen and Allen, 2005).

Idealised models for rift basin development agree on the gross definition and character of these tectono-stratigraphic stages, but they diverge as where to position the syn- to post-rift transition within this framework. Bosence (1998) considers the syn-rift only ends once the rift-related depocentres are filled with sediments and the associated rift topography is "healed"; the top of the syn-rift succession is defined by the post-rift unconformity, which in marginal basins corresponds to the plate breakup. Gawthorpe and Leeder (2000) broadly follow the model of Bosence (1998), and highlight that the final

syn-rift stage (which the authors designate as *fault death stage*) is characterised by an intense erosion of the footwalls, related to the decrease in tectonic activity and the resultant stabilisation of syn-rift drainage systems. Prosser (1993) proposes that the syn-rift ends when the mechanical subsidence associated with rifting ceases (following previous studies of Cartwright, 1991; see also Nottvedt et al., 1995). Consequently, the post-rift includes passive infilling of any relict rift-related relief, and Prosser (1993) does not describe an unconformity between the syn- and post-rift. Morley (2002) highlights the difficulty of defining the end of the syn-rift stage in his model using the observations of Prosser (1993), showing that the sedimentary fill associated with active faulting can have the same stratigraphic architecture (i.e., across-fault thickening) as a succession that simply fills an inactive, sediment-starved hanging-wall.

Determination of the timing and stratigraphic position of the late syn-rift to early post-rift boundary becomes even more complex if one extrapolates the tripartite scheme established for rift basins to rifted margins, given that rifted margins are often associated with: (i) a tectonic transition that is not instantaneous; (ii) net-subsidence that may be punctuated by transient periods of uplift; and (iii) the oceanward migration of strain (e.g. Peron-Pinvidic et al., 2013; Brune et al., 2014; Pérez-Gussinyé, 2020; Chenin et al., 2021). The polyphase rifting model for rifted margins (*sensu* Chenin et al., 2021) defines different domains associated with sequential periods of active deformation, and characterised by specific tectonic structures and related stratigraphic architectures. In this model, the term *syn-rift* refers to the *temporal* dimension of the rift event, i.e., from the onset of crustal extension, to plate rupture and the steady-state emplacement of oceanic crust. This sedimentary sequence can then be subdivided into pre-, syn- and post-tectonic (*sensu* Péron-Pinvidic et al., 2007), based on the architecture of sedimentary deposits with respect to local tectonic structures and their activity. Syn-tectonic sediments are usually

wedge-shaped and associated with a normal fault; whereas post-tectonic deposits are either made of strata downlapping onto, onlapping against or draping residual rift-related topography (Chenin et al., 2021 – see their figure 2).

The marginal basins of southeastern Brazil, including the Campos Basin, have not historically used the tripartite scheme outlined above by Prosser (1993) and others, with the syn- and post-rift intervals instead being subdivided into three tectono-stratigraphic stages: rift, sag and passive margin (or drift) (e.g. Rangel et al., 1994; Winter et al., 2007; Mohriak et al., 2008). Because of the reasons outlined above, there is no consensus on where to position the sag stage within the rifting process. Some authors consider it to be post-rift (Winter et al., 2007; Alvarenga et al., 2021), whereas others position it within the late syn-rift (Karner and Gamboa, 2007; Torsvik et al., 2009). Some authors even argue it constitutes an additional, *transitional stage* between the syn- and post-rift, with the passive margin stage being equivalent to the classically defined post-rift stage (i.e. sediments deposited after breakup has occurred) (Rangel et al., 1994; Beglinger et al., 2012; Cainelli and Mohriak, 1999). Variable interpretations of the tectono-stratigraphic framework of the southeastern Brazilian margin may reflect uncertainties related to the number and origin of rift-related unconformities (especially the breakup unconformity; *sensu* Falvey, 1974). Two (rather than one) erosional unconformities have been recognized in the southeastern Brazilian basins. The first occurs between the rift and the sag stages and is known as the *pre-Alagoas* (or *pre-neo-Alagoas*) unconformity, which is dated at 120 – 123 Ma (intra-Aptian; Winter et al., 2007; Mohriak et al., 2008). Some authors argue that this unconformity records breakup of the South Atlantic continental crust, and that therefore marks the end of the syn-rift (e.g. Cainelli and Mohriak, 1999; Mohriak et al., 2008). A second erosional unconformity occurs between the sag pre-salt sediments and the salt (Winter et al., 2007; Karner and Gamboa, 2007; Alves et al., 2017).

The origin of this unconformity is uncertain; for example, Karner and Gamboa (2007) attribute it to base-level fall, lake desiccation, and subaerial erosion during the late syn-rift, whereas Alves et al. (2017) partially attribute it to a combination of subaerial exposure and shear traction at the base of flowing salt during gravity-driven tectonics, with ridge push-related uplift as an additional tectonic driver.

In this study, we use 2D and 3D seismic reflection and borehole data to characterise the syn-rift tectono-stratigraphic architecture and the geometry and nature of the syn-rift main unconformities in the shallow and deep-water domains of the central Campos Basin, offshore southeast Brazil. We detail three, post-pre-rift intervals – *lower pre-salt*, *upper pre-salt* and *salt* – and their bounding surfaces. We subsequently discuss the origin of these stratigraphic surfaces, and correlate them across the study area. Finally, we define the pre-, syn-, and post-rift tectono-stratigraphic stages within a polyphase rifting model.

## 2. Geological Context

The Campos Basin originated during the rifting process that led to the breakup of Gondwana, culminating with the opening of the South Atlantic Ocean in the Upper Jurassic/Lower Cretaceous (Chang et al., 1992; Szatmari, 2000; Moulin et al., 2010). The basin is located on the southeastern Brazilian margin (Figure 1a). The northern boundary between Campos and Espírito Santo basin is defined by the Vitória High, whereas the southern boundary with Santos Basin is marked by the Cabo Frio High (Figure 1a; Mohriak et al., 1989).

The stratigraphy of the Campos Basin can be broadly divided into three tectono-stratigraphic sequences or megasequences: rift, sag, and passive margin (Figure 1b) (e.g.

Cainelli and Mohriak, 1999; Winter et al., 2007). The rift sequence initiated at c. 135 Ma coeval with intense volcanic activity that emplaced basaltic and volcanoclastic rocks of Cabiúnas Formation, which here are considered part of the basement (Mizusaki et al., 1992; Winter et al., 2007.). The sedimentary sequence of the rift stage (Barremian – early Aptian) comprises the basal and intermediate intervals of the Lagoa Feia Group (Winter et al., 2007), characterised by lacustrine deposits (interbedded with the volcanoclastics of Cabiúnas Formation), including alluvial conglomerates and sandstones, organic-rich shales, and bioclastic rudstones and grainstones (Abrahão and Warme, 1990; Rangel et al., 1994, Goldberg et al., 2017).

Rifting was accommodated by NE-SW-striking normal faults that dip to the NW or SE, and which bound structural highs (horsts) and lows (grabens) (Dias et al., 1988; Chang et al., 1992, Alvarenga et al., 2021), including the Badejo, Intermediate and External highs, and the Corvina-Parati and External lows (Figure 2a; Guardado et al., 2000). The marginal hinge line of the rift system is delineated by the Campos fault (Figure 2a), which separates the shallow western part, where Tertiary deposits rest directly on basement, from the deeper eastern portion, where relatively thick accumulations of Barremian to Aptian sediments fill rift-related depocentres (Guardado et al., 1989).

The sag sequence (upper Aptian) marks the transition from mechanical subsidence, induced by basement-involved faulting and mechanical subsidence, to a period characterised by longer-wavelength subsidence, driven by cooling of the lithosphere, and little normal faulting (Chang et al., 1992; Mohriak et al., 2008). This sequence is dated between 116 – 123 Ma (Karner and Gamboa 2007; Moreira et al., 2007), becoming progressively older from the proximal to distal parts of the basin (Pérez-Gussinýe et al., 2020). The shift in subsidence style is marked by a regional unconformity (*i.e.* the pre-Alagoas unconformity, as named by Guardado et al., 1989; Chang et al., 1992

and Dias et al., 1988). The sag stage comprises the upper Lagoa Feia Group, which is characterised by clastic sediments in proximal parts of the basin, and chemically precipitated carbonates with some microbial influence in more distal areas, which are overlain by a thick layer of evaporites (Figure 1b; Dias et al. 1988; Winter et al., 2007, Lima and De Ros, 2019).

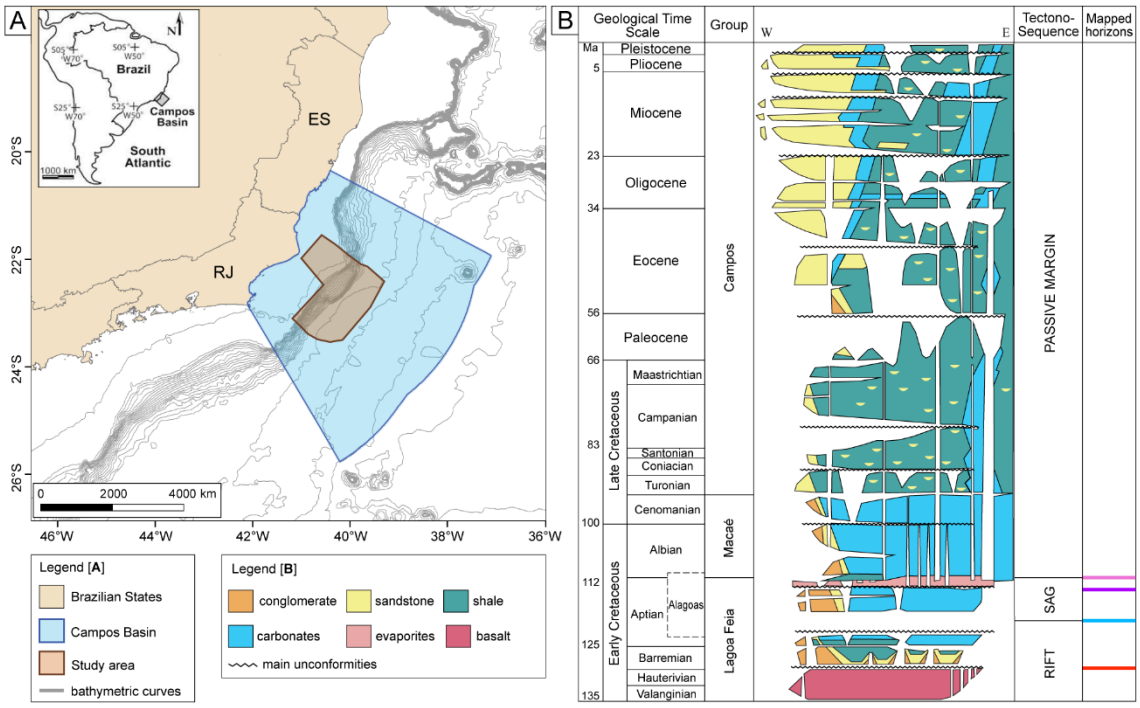


**Figure 1.** (A) Regional map showing the location of Campos Basin and the study area polygon highlighted in brown (B) Simplified stratigraphic chart of Campos Basin, subdivided into three tectono-sequences: rift, sag and passive margin (redrawn from Winter et al., 2007); the column to the right shows the mapped horizons of this study with their designed colours.

SE-tilting of the basin following continental breakup, inducing gravity gliding of the Aptian salt and its overburden (Davison, 2007). Based on the structural style of salt and its overburden, the Campos Basin is divided into three domains of salt-related deformation: (i) a proximal extensional domain, associated with the formation of listric normal faults, rafts, and salt rollers; (ii) a distal contractional domain, characterised by salt-cored anticlines and diapirs; and (iii) an intermediate multiphase domain, dominated by hybrid extensional/compressional structures and ramp syncline basins (Figure 2a; Amarante et al., 2021).

It is important to note that the depositional ages of the pre-salt succession of Winter et al. (2007) (Figure 1B) have been extensively debated. High-resolution carbon isotope data from the eastern Brazilian margin were recently correlated with well-calibrated Tethyan sections by Tedeschi et al. (2019). They presented high-resolution, carbon isotope ($\delta^{13}C$) data from basins along the eastern Brazilian margin, correlating them with well-calibrated Tethyan sections. These new correlations conclude that major evaporite deposition in the South Atlantic occurred in the early Aptian (124 – 125 Ma), suggesting the underlying pre-salt sag sequence is approximately late Barremian and the deeper rift sequence is approximately Hauterivian – lower Barremian (Strugale and Cartwright, 2022 – see their figure 2). However, these new age constraints for the salt were recently challenged by Szatmari et al. (2021), who suggest that the eastern Brazilian basins evolved in a different paleoenvironmental and thus faunal realm to the Tethyan section, meaning a correlation between the two is problematic. Instead, These authors used $^{39}Ar$–$^{40}Ar$ dating to propose that the South Atlantic evaporites (and related volcanic rocks) are c. 116 – 110 Ma (i.e., latest Aptian-earliest Albian).

Plate reconstructions models show that the onset of seafloor spreading in the southern Campos Basin occurred during the late Aptian (c. 115 Ma; Heine et al., 2013; Moulin et al., 2013). This means that the sag sequence (pre-salt and salt) can be either pre-, syn- or post-breakup, depending on whether the age constraints of Tedeschi et al. (2019) or Szatmari et al. (2021) are considered correct. Considering what is most accepted in plate reconstructions, the sag interval is pre- to syn-breakup, with the 'break' in 'break-up' meaning crustal separation (e.g. Heine et al., 2013; Perez-Gussinye et al, 2020; Kukla et al., 2018).

The passive margin sequence marks the start of oceanic spreading and the development of the Mid-Atlantic Ridge (Winter et al., 2007). The initiation of this period

was associated by a marine transgression, recorded by shallow-water carbonate platforms of the Macaé Group (Albian – Cenomanian), overlain by a sequence of pelagic and hemipelagic mudstone and turbidites of the Campos Group (Turonian – Present; Chang et al., 1992). The Macaé and Campos groups are separated by a regional erosional unconformity at 93 Ma (Figure 1b; Guardado et al., 1989).

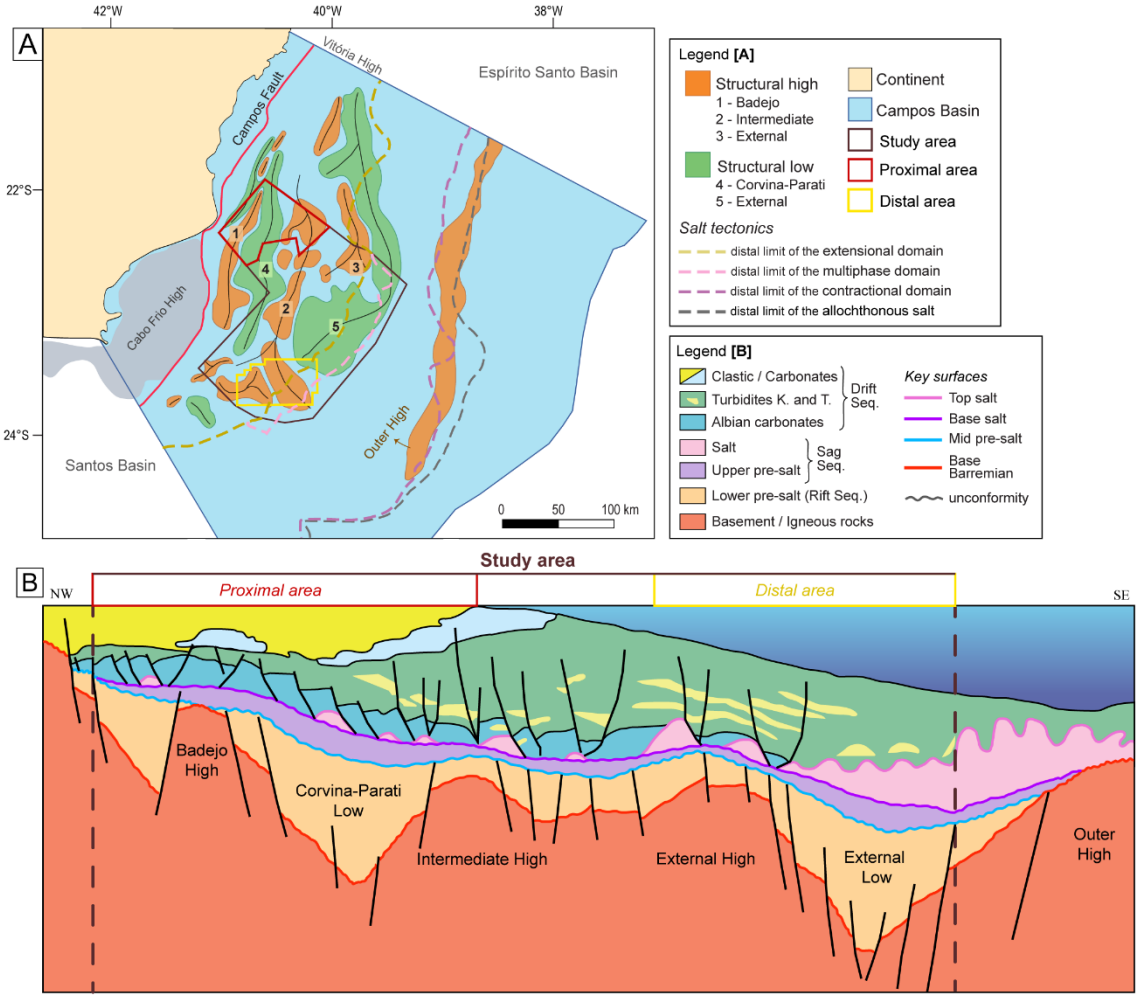


**Figure 2.** (A) Structural framework of Campos Basin. Structural highs and lows are from Guardado et al. (2000); the Outer High and Cabo Frio High locations are from Fetter (2009); and salt tectonics domains from Amarante et al. (2021). (B) Schematic cross section of Campos Basin, showing the rift-related structures present in the detailed proximal and distal portions within the study area (see Figure 3). Redrawn and modified from Rangel et al., 1994.

## 3. Database and Methodology

The database for this study comprises 209 2D seismic reflection lines (or line segments), one 3D seismic reflection volume, and 33 wells from the ANP (Brazil's National Oil, Natural Gas and Biofuels Agency) data library. In total, the 2D seismic surveys cover an area of c. 23,300 km² (Figure 3). The 3D volume covers an area of c. 2,900 km² in the southern part of the study area, with inline (east-west) and crossline (north-south) spacing of 12.5 m. The seismic surveys are time-migrated (PSTM Kirchoff), zero-phase processed, and are displayed with SEG normal polarity, where a downward increase in acoustic impedance is represented by a positive reflection event (white on displayed seismic profiles) and a downward decrease in acoustic impedance is represented by a negative reflection event (black on displayed seismic profiles). All seismic data (lines and maps) are presented in miliseconds (ms) two-way travel time (TWT).

The 33 boreholes include well-logs (e.g. sonic travel time and gamma ray), stratigraphic (age and formation tops) and cuttings-based lithological data, used to constrain the age, composition, and lithostratigraphy of the mapped horizons and the units they bound. These wells were tied to the seismic data through check-shot surveys. The interval velocity of the Aptian evaporites obtained from the well-logs ranges from 4000 – 7000 m/s, depending on the proportion of halite, anhydrite, and potash salts. The sedimentary succession below the salt is defined by interval velocities ranging from 3100 – 6000 m/s due to the varying densities and porosities of the different lithologies (e.g. sandstones, carbonates, mudstones). We estimate that the vertical seismic resolution in the interval of interest is 25 – 50 m; more specifically, 30 – 50 m within the salt (using a dominant frequency of 35 Hz), and 25 – 50 m within the underlying strata (considering a dominant frequency of 30 Hz).

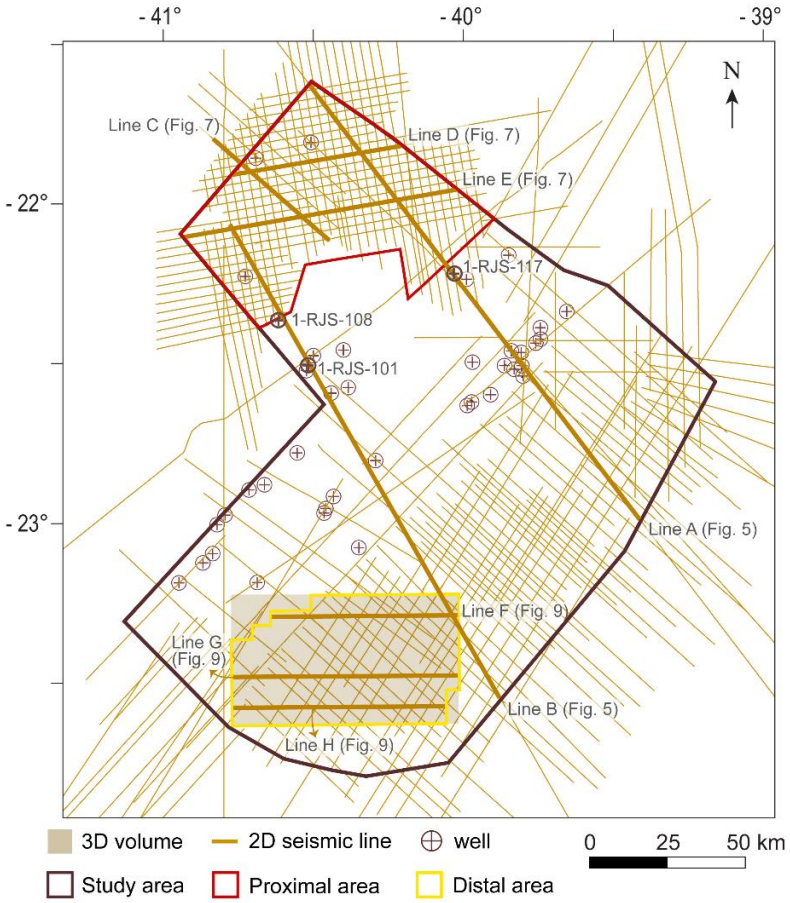


**Figure 3.** Dataset used in this study: 209 2D seismic lines (or lines segments), one 3D volume and 33 boreholes. The red and yellow polygons represent the proximal and distal areas (respectively) which have greater data density.. Note the label of the lines presented in Figures 5, 7 and 9, and the wells 1-RJS-108, 1-RJS-101 and 1-RJS-117 presented in Figure 5.

We identified four key stratigraphic surfaces in the study area, with age constraints provided by well data: base Barremian (top of Cabiúnas Fm.), mid Aptian unconformity (mid pre-salt), late Aptian unconformity (base of the salt), and top Aptian (top of the salt). The last three were mapped across the entire dataset (Figure 1b). We also selected two areas with greater data density and quality, one proximal and one distal (Figure 3), where we mapped the base Barremian (top of Cabiúnas Fm.) surface. The four mapped horizons bound three intervals: *lower pre-salt*, *upper pre-salt* and *salt*. The mapped surfaces display the present basin geometry, whereas isochron maps derived from these surfaces reflect the relative thickness of the intervals. The latter are used to infer temporal and spatial changes in subsidence and accommodation, which might be related to a combination of tectonics, lake-level change, and sediment supply (Figures 4, 6 and 8).

The absolute thickness values presented in the text were calculated by converting time (TWT, ms) to depth using velocities of 4700 m/s and 5100 m/s – i.e. the average interval velocity of the pre-salt and salt intervals, respectively, calculated from the well-logs and check-shots. We also calculated the dip-angle of the mid-pre-salt and base-salt surfaces using the same methodology.

# 4. Results

## 4.1. Basement structures

For the purpose of our study, we consider the basalts of Cabiúnas Formation as part of the basement. The study area comprises the following basement structures, from the proximal to the distal portions: the Badejo High, the Corvina-Parati Low, the Intermediate and External highs, and the External basement low (Figures 2 and 5). These structures are grabens and horsts bounded by N-S- to NE-SW-striking, rift-related normal faults, which dip landward (i.e., to the W/NW) or seaward (i.e., E/SE). The External High is present only in the northeast portion (Figures 2a, 5a).

The proximal area contains the Corvina-Parati Low and the Badejo and Intermediate highs, which are both bounded by N-S- to NE-SW-striking normal faults that are up to 55 km along strike and that have throws of up to 1500 ms TWT. The Corvina-Parati Low is limited to SE by the Intermediate High and to the northwest by the Badejo High, which extends north-westwards until the Campos Fault, the marginal hinge line of the basin (Figures 6a and 7). The Corvina-Parati Low contains two depocenters, which have mean depths between -3500 and -5000 ms TWT, and which are dissected by the Badejo High (Figures 6a and 7). The Badejo High is not as deeply buried as the Intermediate High (c. -3050 to -1600 ms TWT compared to, c. -3700 ms to -2900 ms TWT; Figure 6a).

The distal area contains the External High to the west and the External Low to the east, bounded by N-S- to NNE-SSW-striking normal fault, that are up to c. 40 km long and have throws of up to 800 ms TWT. The External High varies in depth between -4600 and -5800 ms TWT (Figure 8a) and it contains a series of normal faults with relatively small vertical displacement (up to 400 ms TWT), delimiting restricted, asymmetric depocenters (Figure 9). The base of the External Low ranges between -6800 and -7400 ms TWT (Figure 8a), and it contains a series of seaward- and landward-dipping faults that define depocenters separated by internal basement highs (Figure 9b,c).

### 4.2. Lower pre-salt

The base-Barremian horizon separates the chaotic reflections of the basement and syn-rift volcanics (which we are not able to differentiate) from divergent to subparallel reflections of the sedimentary succession (Figure 5). The top of this interval is defined by an erosional unconformity (known in the literature as pre-Alagoas unconformity) that is best-developed near basement highs, and which is characterised by truncation of tilted reflections (Figures 7 and 9).

The base-Barremian in the proximal area varies in depth from -1650 to -4900 ms TWT (Figure 6a). Sedimentation in this interval is mainly restricted to two largely isolated depocentres, named the Corvina-Parati Low. The depocenter to the NW is a relatively symmetric graben, containing high-frequency reflections that occur as a wedge-shaped package that thickens towards the southeastern border fault (Figure 7). The depocenter to the SE is also a symmetric graben, containing subparallel, lower frequency reflections (Figure 7). On the Intermediate High are isolated, asymmetric depocentres containing divergent reflections to NE (Figure 7c).

The base of the Barremian in the distal area varies between -4450 and -7300 ms TWT depth (Figure 8a). Similarly to the proximal area, sedimentation is restricted to isolated depocenters that are isolated from adjacent ones by elevated basement structures. Within grabens and half-grabens of the External Low, reflections are divergent to subparallel, locally folded and disrupted, and have relatively high frequencies and medium to high amplitude. In restricted depocentres within the External High, the reflections are divergent to subparallel, and are of low to medium amplitude and of relatively low frequency (Figure 9).

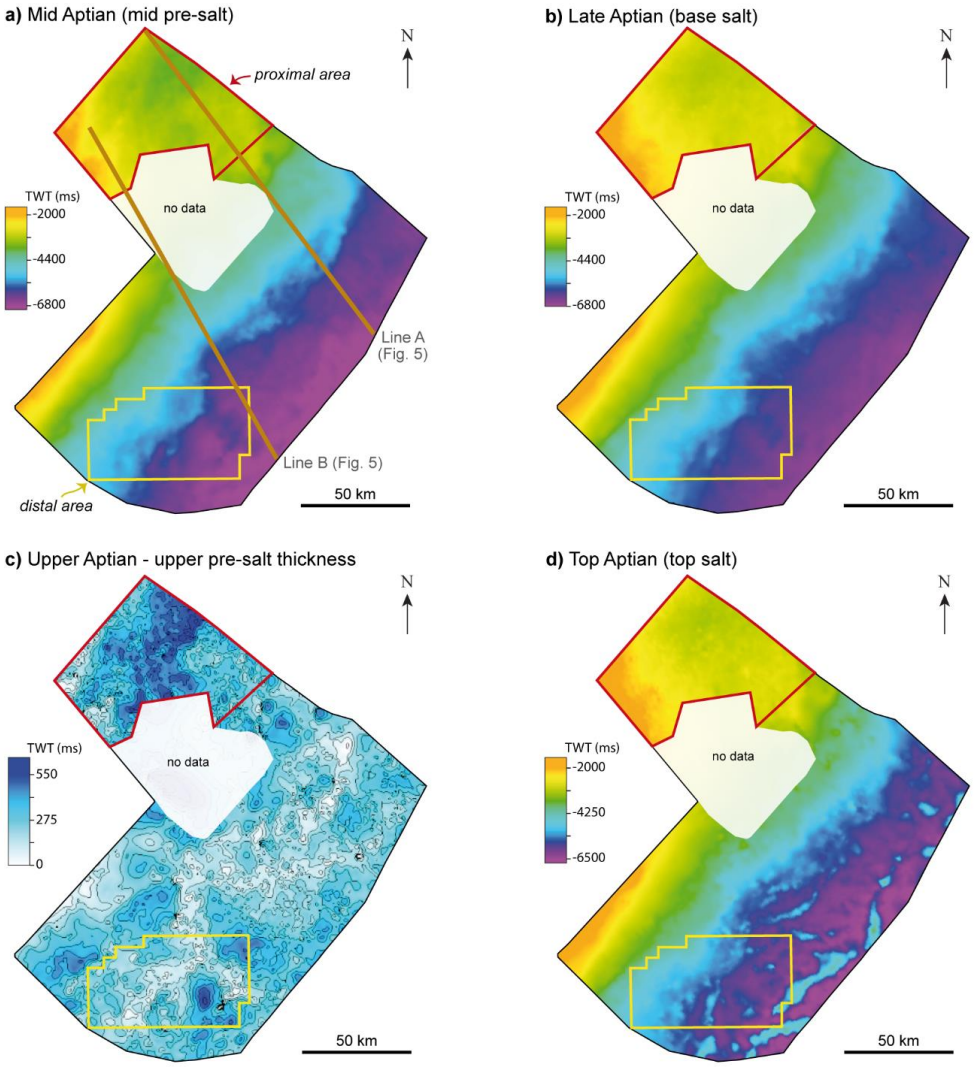


**Figure 4.** Time map of the mid Aptian (mid pre-salt) (a) and late Aptian (base salt) (b) surfaces of the entire study area, respectively, and dip regionally to SE. The seismic lines shown in Figure 5 are indicated in brown. c) Upper pre-salt (Upper Aptian) isochron thickness map, showing values from 0 – 675 ms (TWT); thickness is overall greater in the proximal area (red polygon). d) Time map of the top Aptian (top salt) surface, varying from -1500 and -6700 ms (TWT). The area with very few data (see Figure 3) is indicated in white.

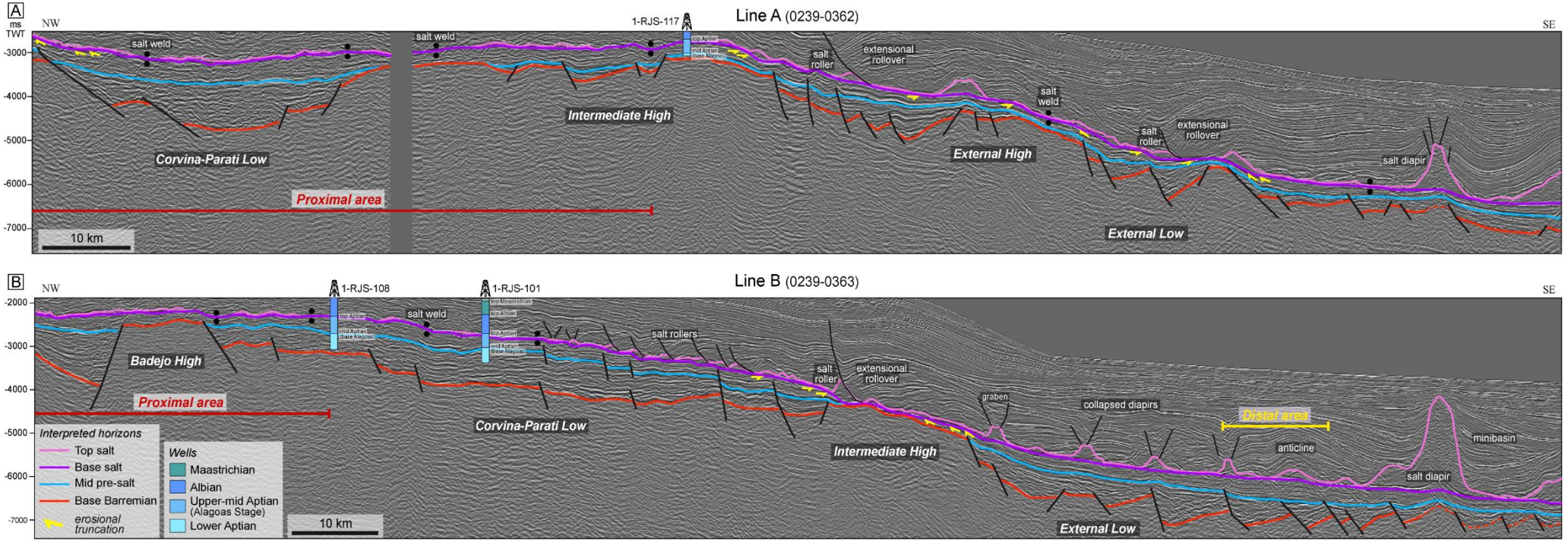


**Figure 5.** Regional lines of the study area (see Figures 3 and 4a for location). The interpreted horizons are indicated in the legend in the lower left corner. Reflection terminations in erosional truncations are highlighted with yellow arrows. There are three wells with age constraints, 1-RJS-117 intersected by Line A, and wells 1-RJS-0108 and 1-RJS-0101 intersected by Line B. The main salt and overburden structures are labelled in pink. The basement highs and lows (see Figure 2) are labelled, as well as the proximal and distal areas.

### 4.3. Upper pre-salt interval

The basal surface varies in depth between -1600 and -7000 ms TWT and dips regionally to SE (Figure 4a); within basement lows, this surface is defined by a continuous reflection that onlaps locally against the larger basement highs or normal faults (Figure 5). The upper pre-salt thickness ranges from 0 – 675 ms TWT (c. 0 – 1580 m), and it is overall greater in the proximal portion (Figure 4c). In general, the reflections within this interval are subparallel and relatively continuous (Figure 5).

In the proximal area, the basal surface varies in depth from -1700 to -3800 ms TWT, and has a mean dip of c. 3.5° to SE. The upper pre-salt thickness in the proximal area varies from 0 to 670 ms TWT (c. 0 – 1570 m) (Figure 6d). At the base of the succession, the reflections onlap onto the basement highs or the base pre-salt surface. The external geometry of this succession is lenticular, thinning towards the basement highs and thickening within the lows (i.e. a sag geometry) (Figure 7). The internal reflections are overall parallel to subparallel, except towards the west where they slightly diverge towards the center of the basin between the Badejo High and the Corvina-Parati Low (Figure 7b).

In the distal area, depth of the basal surface ranges from -4300 to -6900 ms TWT, and has an average dip of c. 4° to SE (Figure 8b). The upper pre-salt thickness in the distal area varies from 0 to 570 ms TWT (c. 0 – 1340 m) and is greatest within the External Low (Figure 8d). The reflections are mostly continuous and parallel to subparallel, but divergent reflections are also present towards some of the normal faults (see numbered faults in Figure 9). The base of the succession is characterised by onlaps onto the basement highs or the basal surface (Figure 9).

### 4.4. Salt – Pre-salt horizon

The base-salt surface lies between a depth range of -1550 to -6800 ms TWT, dipping regionally towards the SE (Figure 4b). The base-salt surface is rugose, defined by a high-amplitude continuous reflection, underlain by either parallel or tilted reflections; in the latter, the base-salt surface defines an erosional unconformities (Figure 5). Between the Intermediate/External highs and the External Low, where the surface is erosional, it is best-described as a downcutting erosional unconformity, i.e., underlying reflections are gently dipping, with the overlying erosional surface cutting down into them more steeply (Figure 5).

In the proximal area, the depth of the base-salt surface ranges between -1600 and -3500 ms TWT of depth, and dips c. 2.5° to SE (Figure 6b,c). The salt – pre-salt contact is defined by an erosional unconformity, especially on basement the Badejo High (Figures 7 and 10a). On the Intermediate High and the Corvina-Parati Low, concordant reflections dominate and the base-salt surface is apparently conformable, at least at the scale of observation permitted by the seismic reflection data. Erosionally truncated reflections locally define channel-like features in the top pre-salt (Figure 10a3) or small incisions at base-salt surface (Figure 10 a2), but the truncated reflections are mostly towards the basement high (Figures 7 and 10 a4). Locally there are truncations within basement lows, in general related to minor faulting (Figure 10a1). The magnitude of erosion at the base-salt increases towards basement highs where the pre-salt is relatively thin and locally absent (Figure 6d).

In the distal area, the depth of the base-salt surface ranges from -3900 to -6400 ms TWT, and has an average dip of c. 3.5° towards SE (Figure 8c). In a similar manner to that observed in the proximal area, the salt – pre-salt contact can defines a downcutting erosional unconformity on basement highs (Figure 9a to the W and Figure 10 b4 to N),

apparently passing laterally into a conformity in adjacent lows (Figures 9 and 10b). Figure 10 b3 shows a channel-like incision measuring 4.5 km, 250 ms TWT high. In a way similar to that observed in the proximal area, the magnitude of erosion at base-salt increases towards the basement highs (Figures 9 and 10 b1, b4).

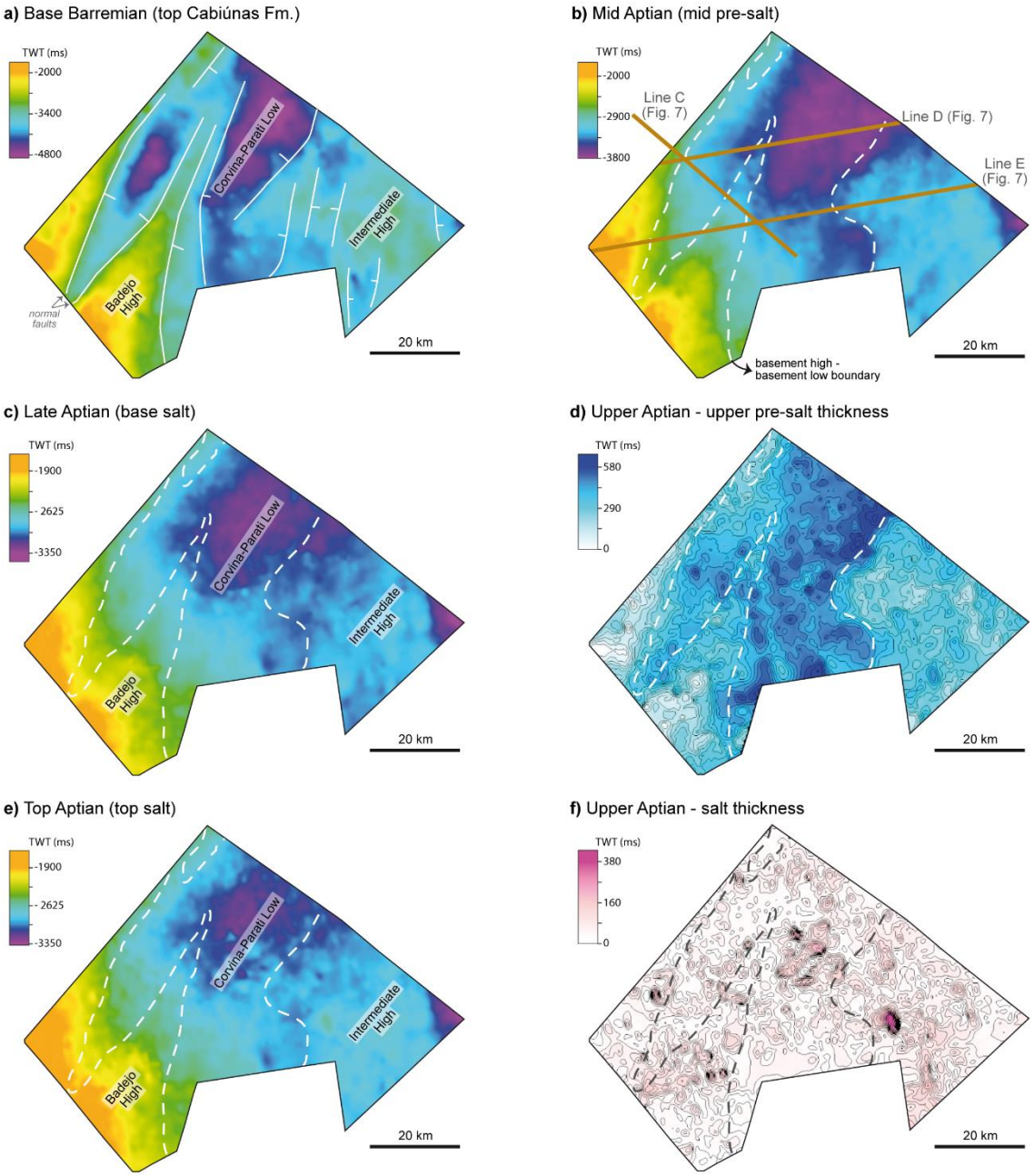


**Figure 6**. Time maps of the proximal study area. a) Time map of the base Barremian (top Cabiúnas Formation) surface; normal faults delineated in white define basement highs (Badejo and Intermediate) and low (Corvina-Parati) – see Figure 2. b) Time map of the mid Aptian (mid pre-salt) surface. The seismic lines shown in Figure 7 are indicated in brown. c) Time map of the late Aptian (base salt) surface. d) Upper pre-salt isochron thickness map, with values up to 670 ms (TWT), greater in the Corvina-Parati basement low in comparison to the basement highs. e) Time map of the top Aptian (top salt) surface. f) Salt isochron thickness map, with values ranging from 0 to 425 ms (TWT) defining salt welds and salt structures. The white/black dashed lines contour basement highs and lows.

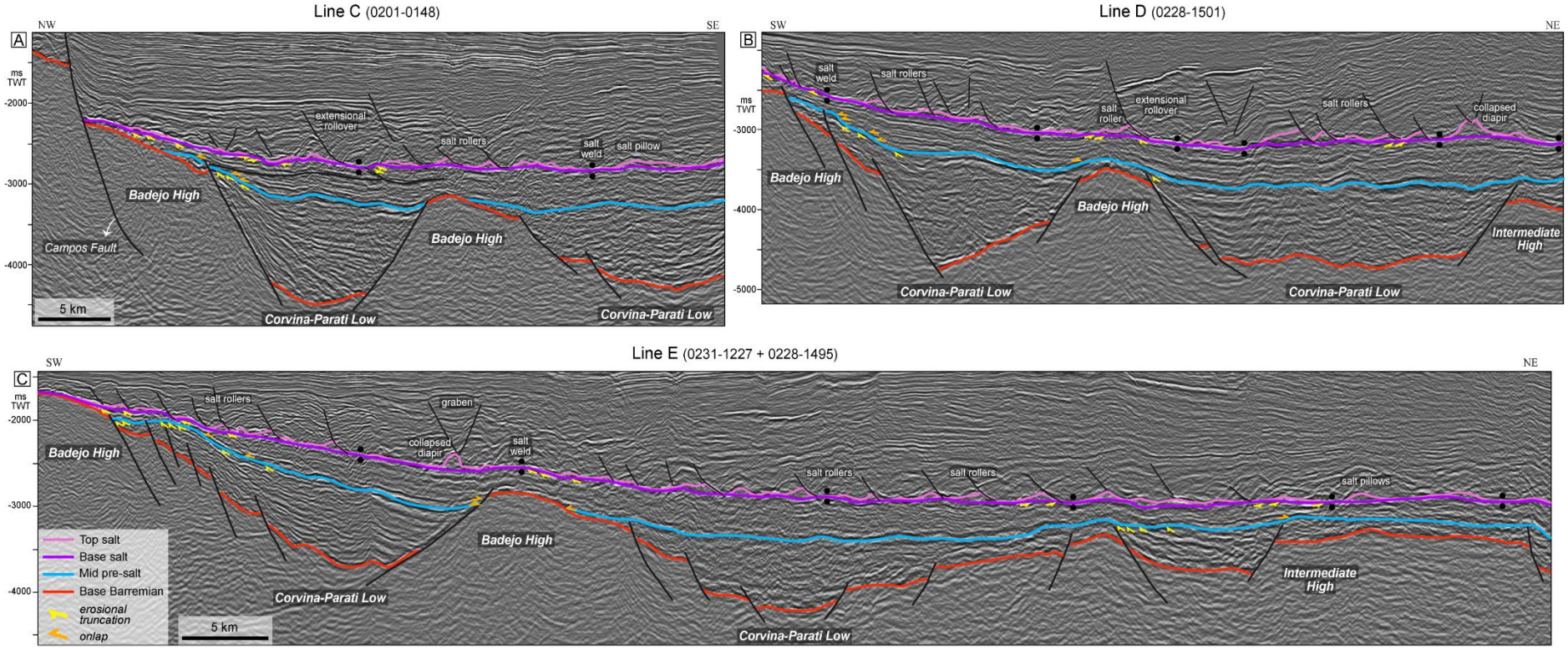


**Figure 7**. Interpreted lines segments of the proximal area within the study area (see Figures 3 and 6b for location of the lines). The interpreted horizons are indicated in the legend in the lower left corner. The main salt and overburden structures are labelled in pink. Reflection terminations in erosional truncations and onlaps are highlighted with yellow and orange arrows, respectively; note how they concentrate to the west, towards the marginal hinge line of the rift system.

### 4.5. Salt

The top salt surface ranges in depth from -1500 to -6700 ms TWT, and it dips regionally to SE (Figure 4d). The morphology of the top salt surface is related to a range of salt structures, including rollers, pillows, diapirs, and anticlines, and numerous related overburden structures such as extensional rollovers, grabens, normal faults, ramp-syncline basins, anticlines, and minibasins (Figures 5, 7 and 9). Salt structures are flanked by salt welds (i.e., areas of relatively thin, depleted salt), where sub- and supra-salt strata appear to be in direct contact. The distribution and structural style of salt and its overburden, and the geometry of related growth strata preserved within ramp-syncline basins, document substantial horizontal translation (i.e., 28 km; Amarante et al., 2021; see also Dooley et al., 2017).

In the proximal area, the top-salt surface varies in depth from -1550 to -3400 ms TWT (Figure 6e). Salt is relatively thin in this area (0 – 100 ms TWT or c. 0 – 250m), being thickest (up to 425 ms TWT or c. 1080 m) in a few, relatively isolated salt structures such as rollers, or more rarely pillows and collapsed diapirs. The salt isochron map shows that the structures are either circular or elongated with a NE to N trend (Figure 6f). Salt structures are typically associated with normal faults overlain by extensional rollovers and/or collapsed grabens (Figure 7).

In the distal area, the top-salt surface ranges between -3900 and -6350 ms TWT in depth (Figure 8e). Salt thickness is highly variable in this area, 0 – 2500 ms TWT (c. 0 – 6375 m) (Figure 8f). The mapped salt structures trend broadly NE to N, sub-parallel to the underlying rift structures (Figure 8a,f). Over the External High, the salt formed rollers and collapsed diapirs associated with normal faults that define grabens and extensional turtle anticlines in the overburden (Figure 9). Structures above the External Low include salt anticlines, rollers, and diapirs (Figure 9).

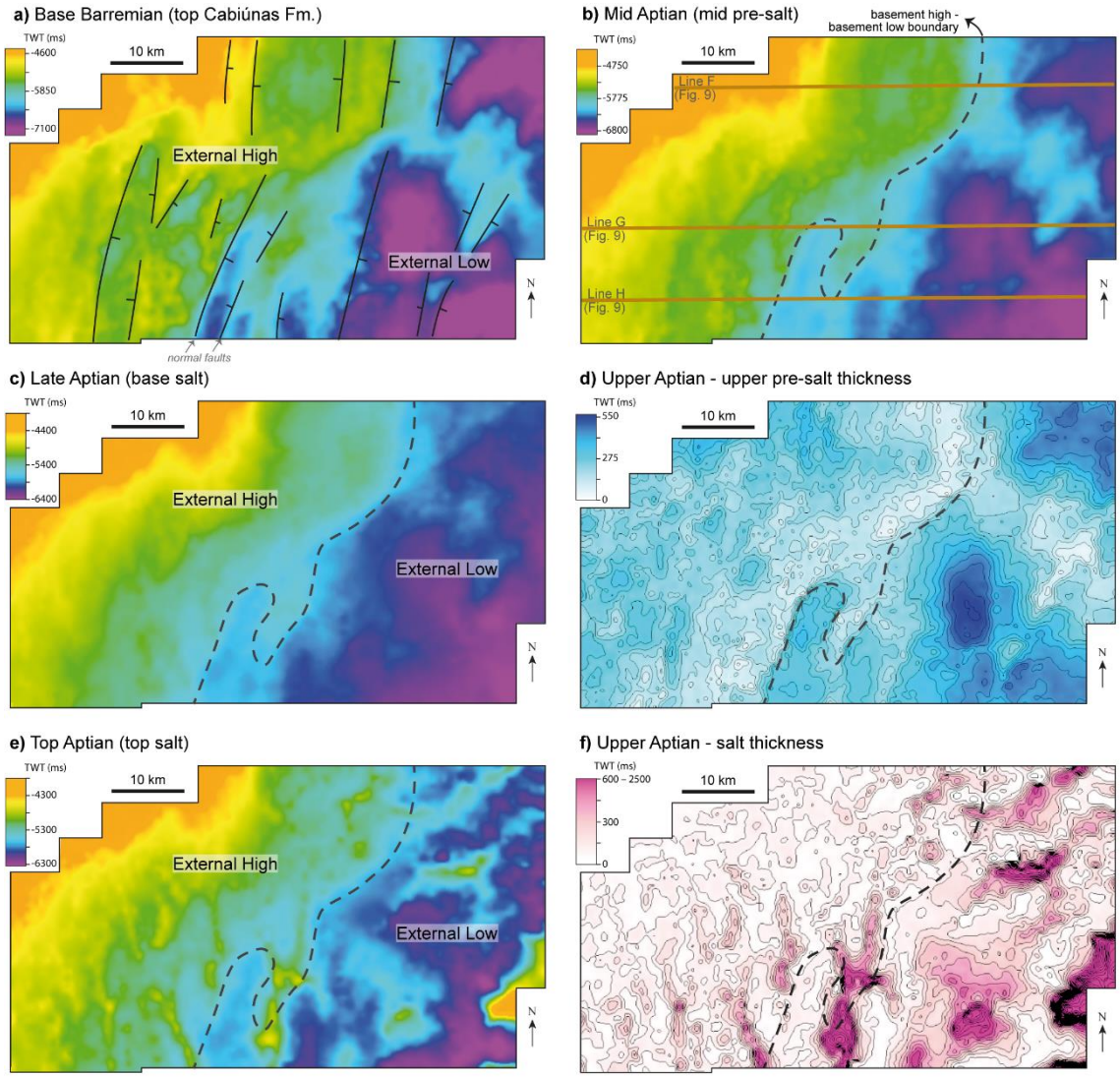


**Figure 8**. Time maps of the distal study area. a) Time map of the base Barremian (top Cabiúnas Formation) surface; normal faults delineated in black define the basement External High and External Low – see Figure 2. b) and c) are time maps of the mid Aptian (mid pre-salt) and late Aptian (base-salt) surfaces. The seismic lines shown in Figure 9 are indicated in brown. d) Upper pre-salt isochron thickness map, with values up to 570 ms (TWT), greater in the External Low in comparison to the External High. e) Time map of the top Aptian (top salt) surface. f) Salt isochron thickness map, with values ranging from 0 to 2500 ms (TWT) defining salt welds and salt structures. The black dotted line bounds the basement high and low.

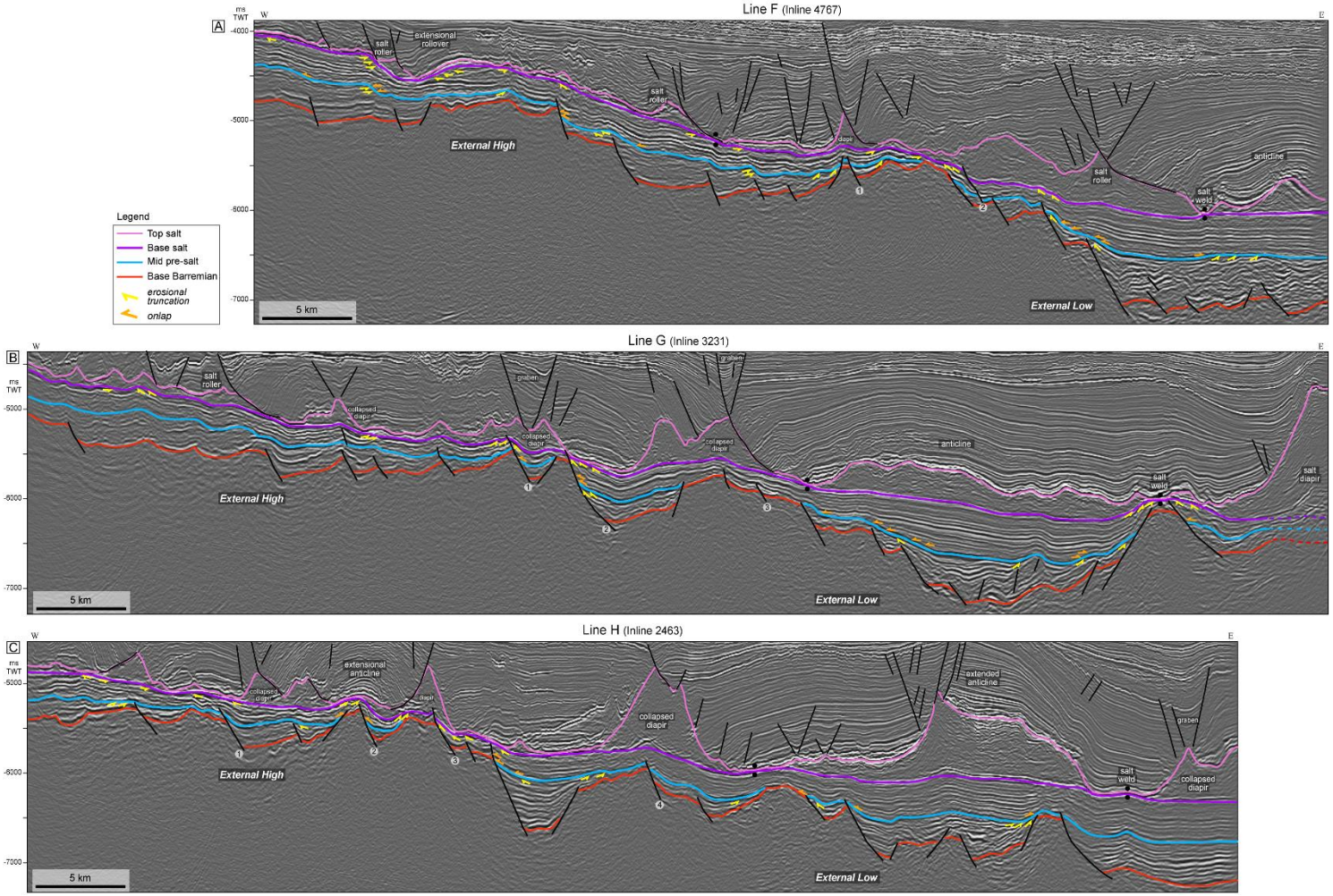


**Figure 9**. Interpreted lines of the distal area (3D volume) within the study area (see Figures 3 and 8b for location of the lines). The interpreted horizons are indicated in the legend in the lower left corner. The main salt and overburden structures are labelled in pink. The faults that were active during the upper pre-salt interval are numbered. Reflection terminations in erosional truncations and onlaps are highlighted with yellow and orange arrows, respectively; note how they concentrate to the west, in the External High and in the boundary between the External High and the External Low. In (b) and (c) there are also erosional truncations near the internal basement high to the east.

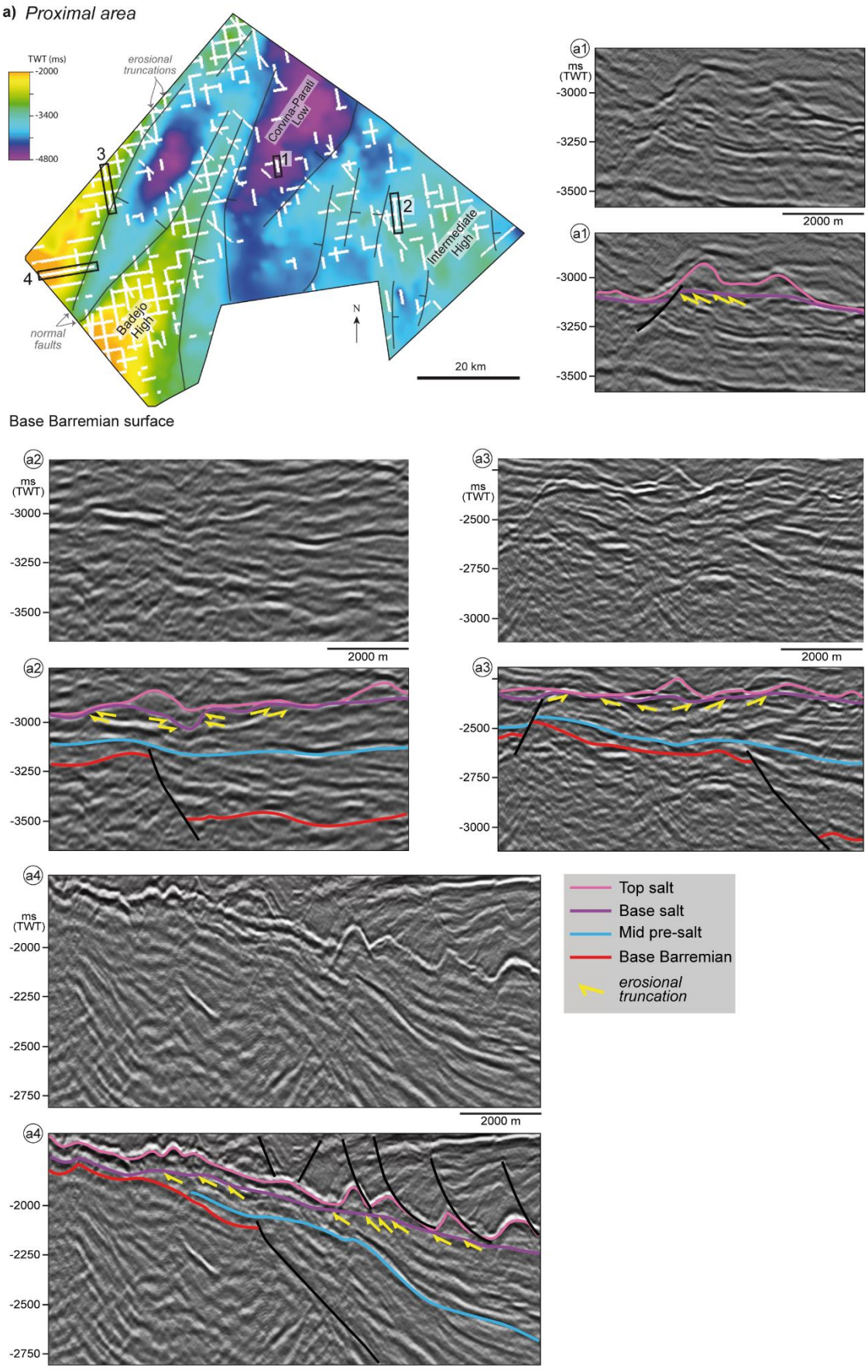
a) Proximal area
TWT (ms)
-2000
-3400
-4800
erosional truncations
Corvina-Parati Low
Intermediate High
Badejo High
normal faults
N
20 km
Base Barremian surface
a1
ms (TWT)
-3000
-3250
-3500
2000 m
a2
-3000
-3250
-3500
a3
-2500
-2750
-3000
a4
-2000
-2250
-2500
-2750
Top salt
Base salt
Mid pre-salt
Base Barremian
erosional truncation

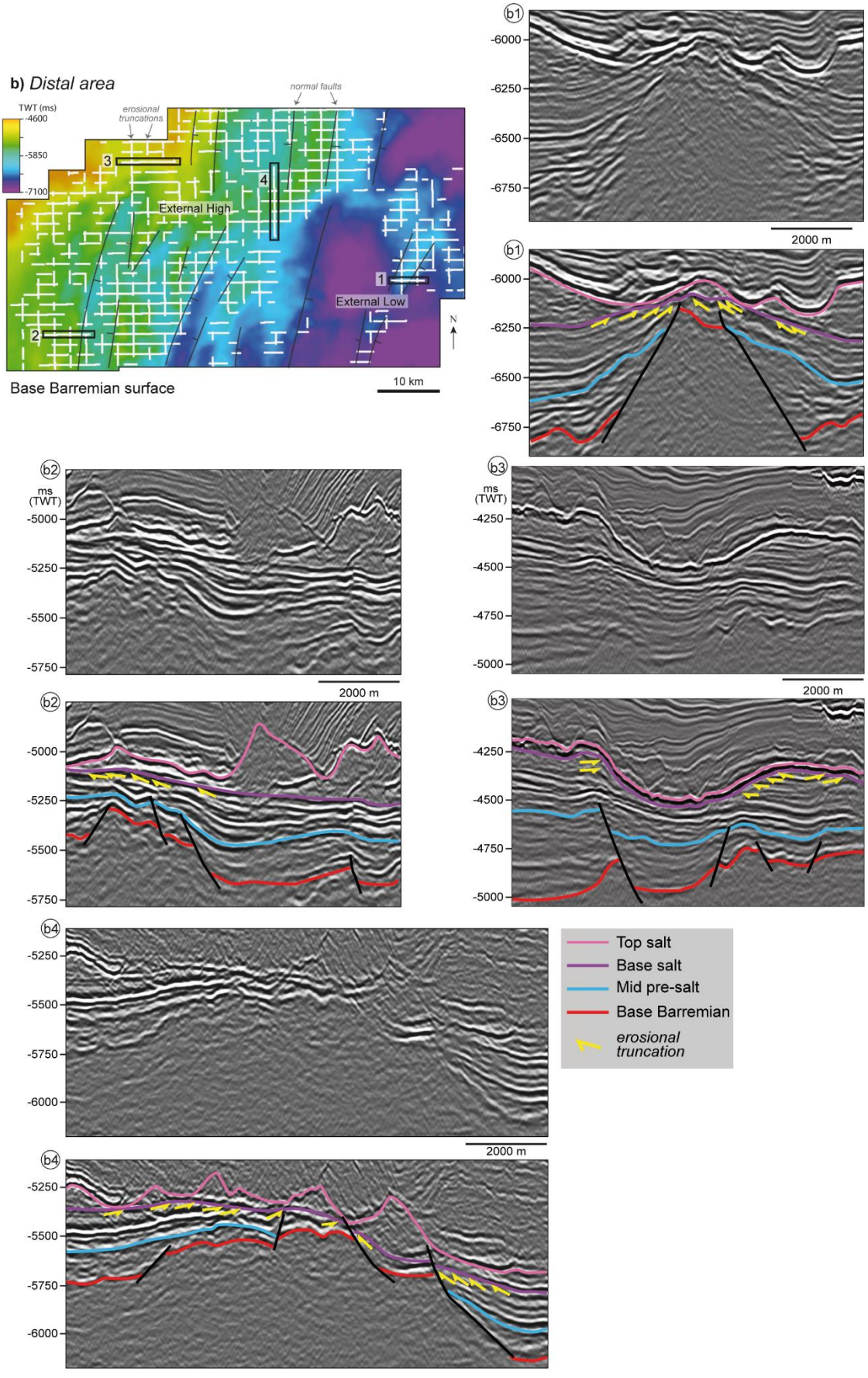
b) Distal area
normal faults
TWT (ms)
-4600
-5850
-7100
erosional truncations
3
4
External High
1
External Low
2
N
Base Barremian surface
10 km
b1
-6000
-6250
-6500
-6750
2000 m
b2
ms (TWT)
-5000
-5250
-5500
-5750
b3
-4250
-4500
-4750
-5000
b4
-6000
Top salt
Base salt
Mid pre-salt
Base Barremian
erosional truncation

*(previous pages)* **Figure 10**. Time map of the base-rift (top Cabiúnas Formation) surface in the proximal (a) and distal (b) areas, with series of erosional truncations mapped in white. Numbers 1 to 4 are segments of seismic lines to best show the reflection terminations, highlighted in yellow arrows when they are erosional truncations.

# 5. Discussions

## 5.1. Expression and development of unconformities in the Campos Basin

In this section, we discuss the possible age, origin, and significance of the three key seismic-scale stratigraphic surfaces identified below Aptian salt in the Campos Basin.

### 5.1.1. *Base-Barremian surface*

The base-Barremian surface dates c. 130 Ma, and separates the volcanics of Cabiúnas Fm. and pre-rift basement rocks from early syn-rift sedimentary strata (Winter et al., 2007) (Figures 1, 2 and 5). This surface post-dates the syn-rift unconformity (*sensu* Bosence, 1998) or rift onset unconformity (*sensu* Falvey, 1974), located either within or at the base of the Cabiúnas Formation (Goldberg et al., 2017).

### 5.1.2. *Mid-pre-salt unconformity*

The mid-pre-salt unconformity separates the lower and upper pre-salt units. The character of the surface changes spatially from an erosional unconformity above the highs to a conformity away from them, over the rift depocentres (Figures 7 and 9). The mid-pre-salt is described as an angular unconformity, separating divergent and locally deformed reflections of the lower pre-salt from subparallel reflections of the upper pre-salt. This unconformity has been previously documented in the Campos, Santos and Espírito Santo basins, where it was referred to as the *pre-Alagoas* (or *pre-neo-Alagoas*) unconformity (c. 120 – 123 Ma) (Guardado et al., 1989; Winter et al., 2007; Mohriak et

al., 2008). Our well data show that this surface coincides with the base of the Alagoas Stage (123 Ma) (Figure 5), a local stage within the Early Cretaceous (Figure 1b).

Some authors argue that the pre-Alagoas unconformity corresponds to the breakup unconformity (e.g. Cainelli and Mohriak, 1999; Mohriak et al., 2008), which Bosence (1998) positions at the syn- to post-rift contact. This interpretation leads to the classification of the upper Aptian of the southeastern Brazilian basins as *transitional* (i.e. between the syn- and post-rift) or *post-rift* (e.g. Rangel et al., 1994; Cainelli and Mohriak, 1999; Beglinger et al., 2012; Alvarenga et al., 2021). The term *breakup unconformity* as defined by Falvey (1974) is an erosional surface, originating from the uplift of rift flanks at the time of breakup, and synchronous with the onset of oceanic crust accretion. This unconformity is typically described as being erosional, truncating underlying, wedge-shaped, syn-rift strata, separating them from younger post-rift sequences that show little to no evidence of fault-controlled deposition (Braun and Beaumont, 1989; Franke, 2013). The breakup unconformity thus represents the cessation (or decrease) of rift-related tectonic subsidence, and the onset of a long-wavelength, relatively slow subsidence driven by post-rift cooling of the newly formed oceanic crust (Hiscott et al. 1990).

More recently, polyphase models of continental breakup have been developed using a combination of observations from new, higher-resolution geophysical data imaging the distal parts of rifted margins, and now-exhumed and exposed ancient margins. These models argue that the process of continental breakup is unevenly distributed in time and space, and thus is not recorded by a single surface (or reflection) that is age-equivalent across the proximal and distal domains of rifted margins (e.g. Peron-Pindivic et al., 2013; Brune et al., 2014; Pérez-Gussinyé, 2020; Chenin et al., 2021). According to Pérez-Gussinyé et al. (2020), on weak asymmetric margins such as the Angola/Northern Campos-Espirito Santo conjugates, the breakup event is only

recorded as an unconformity in areas affected by deformation related to final crustal rupture (i.e. the most distal part of the margin). This means that the cessation of tectonic subsidence does not occur simultaneously across the entire margin, and thus it does not generate a basin-wide response recorded as a stratigraphic marker across the entire basin. Instead, margin breakup generates local flexural rebounds in response to elastic stress drop linked with progressive faulting and thinning (Pérez-Gussinyé et al., 2020). Chenin et al. (2021) state that not all unconformities within rift basins mark the beginning of the post-rift. For example, the proximal domains of rifted margins may contain unconformities related to local or large-scale tectonic events, or due to climatic events or changes in sea- and/ or lake-level (Prosser, 1993). Previous studies also show that rather than a rapid tectonic event, lithospheric breakup reflects a gradual process where exhumation and extension of the exhumed mantle (and continental crust) and embryonic oceanic crust accretion may overlap until the latter dominates (Sibuet et al., 2007; Jagoutz et al., 2007).

We argue that the mid-pre-salt (or *pre-neo-Alagoas*) unconformity predates and is, therefore, not related to the breakup event associated with formation of the South Atlantic in the south-central Campos Basin; this interpretation is consistent with other studies of marginal basins of SE Brazil (e.g. Karner and Gamboa, 2007; Torsvik et al., 2009; Araujo et al., 2022). We instead interpret that this surface is a *rift migration unconformity* (*sensu* Pérez-Gussinyé et al., 2020) formed when deformation across a given fault block (and slip on its bounding faults) ceases and migrates oceanward. This generated an angular unconformity separating syn- and post-tectonic strata, rather than syn- and post-rifting strata (*sensu* Péron-Pinvidic et al., 2007), marking the onset of a sag-type basin. Even though the mid-pre-salt unconformity is identified in both the proximal and distal areas of south-central Campos Basin, its formation is diachronous across the

basin, reflecting the oceanward migration of deformation (Ranero and Pérez-Gussinyé, 2010; Pérez-Gussinyé et al., 2020). In our study area, this unconformity marks the end of fault activity, although, in the distal area a number of rift-related faults remained active locally after its development (numbered faults in Figures 9 and 11). Araujo et al. (2022) also documented the mid-pre-salt unconformity in the neighboring Santos Basin (which the authors named Mid Aptian Synrift Unconformity). The authors show this surface separates syn-tectonic sediments below from sediments deposited in sag-like geometry above in the proximal margin of Santos Basin; in the distal margin (further oceanward than the distal area of our study), the sag-like geometry changes to typical syn-rift, syn-tectonic structures, providing evidence for continuing rift migration. Chenin et al. (2015) uses the term *necking unconformity* for the transition from syn- to post-tectonic deposits. The unconformity described here could be interpreted as the necking unconformity and may thus record a period of substantial but more localized crustal thinning (Peron-Pinvidic and Manatschal, 2009; Mohn et al., 2010).

#### 5.1.3. *Base-salt unconformity*

The contact between the salt and the pre-salt strata is rugose in most parts, being underlain by either concordant or truncated reflections (Figures 7, 9 and 10). This unconformity is regional, being better developed on basement highs across the margin. Between the Intermediate/External highs and the External Low, the unconformity is locally expressed as a downcutting erosional unconformity (Figure 5), which indicate either: (1) vertical erosion into sub-horizontal strata or, perhaps more likely given the tectonic history of the margin; (2) the External Low tilted oceanward after salt deposition, meaning this is an *apparently* downcutting erosional unconformity that originally formed by erosion of already tilted strata.

Within basement lows, concordant reflections dominate, but there are some truncations (especially in the proximal area) that due to their spatial restriction are likely associated to either: (1) normal faults that were active prior to salt deposition (Figures 7a and 10 a1); or (2) more speculatively, lacustrine wave erosion (where the is no fault near the erosion, e.g. Figure 7b to NE).

The salt – pre-salt contact is classified as an unconformity given the regional character of the surface, and based on the fact it defines an abrupt shift in depositional environment from shallow lacustrine to a restricted marine system (Winter et al., 2007). The period of erosion and nondeposition related to this surface is uncertain, due to the debate around the age of evaporite deposition. If we consider the age of the evaporites by Szatmari et al., (2021), of c. 110 – 116 Ma and an estimated duration of evaporite deposition of c. 0.5 Ma – based on correlation of the main evaporite sequences to Milankovitch cycles by Freitas, (2006) and on the comparison to known evaporite depositional rates in different salt basins by Davison et al. (2012) –, base-salt unconformity can comprehend a time gap of c. <0.1–6.0 Ma.

Alves et al. (2017) documented base-salt erosion in the Santos Basin. These authors attribute this erosion to three factors, depending on the structural position on which it is observed. For example, on structural highs, similar to what we observed in our study, Alves et al. (2017) associate erosion with sub-aerial exposure. In contrast, at some distance (up to 20 km) from structural highs they attribute erosion to either (1) thick-skinned tectonics that caused diachronous reactivation and inversion of rift-related normal faults; or (2) drag (i.e., friction) along the top of the sub-salt strata where it is in contact with the overriding, basinward-flowing salt. They propose that the latter mechanism is specifically relevant where the top pre-salt is flat and subsalt strata are strongly eroded (see their figure 9). Alves et al. (2017) also quantified the magnitude of

base-salt erosion, suggesting this locally exceeded 20% (c. 62 m) of the pre-salt Aptian carbonate original thickness (313 m – Moreira et al., 2007). To derive this value the authors use the method of Roberts and Yielding (1991), where reflection truncations are mapped across eroded half-grabens and projected upwards following a tabular and regular geometry (see their figure 6). A key question that arises from this interpretation is "does basinward-flowing salt have sufficient mechanical strength to erode large volumes of underlying material, which in the case of Campos and Santos basins are lithified carbonates?".

There are two end-members of flow regimes for salt; Poiseuille and Couette (e.g Rowan et al., 2004; Weijermars et al., 2014; Fossen, 2016; Sarkarinejad et al., 2018). Poiseuille flow is driven by a lateral pressure gradient within the salt; in this case, overburden strata that load the salt and drive deformation may subside into the salt, but it does not move horizontally. Couette flow is dominated by shear stress and occurs when the sedimentary overburden glides down a gentle slope. In nature, it is likely that salt flow is a mix of both (i.e. hybrid Couette-Poiseuille flow; e.g. Sarkarinejad et al., 2018 - see their figure 1). In all three flow regimes (Couette, Poiseuille and hybrid), the salt velocity during horizontal translation is null at the base-salt, meaning the salt (and overburden) movement is decoupled from the underlying strata and, we argue, cannot therefore erode it. Furthermore, if salt had eroded the underlying rocks, there should be evidence of pre-salt-derived clastics and carbonates within the salt. We see no evidence of this, at least at the seismic-scale. Finally, in the Campos Basin there is no relation between the style of salt and overburden structures and upper pre-salt erosion. More specifically, rather that intra-salt and overburden shortening structures being restricted to subsalt highs (see Alves et al., 2017), areas with pronounced pre-salt erosion are characterised by extensional salt structures (Figures 7 and 9) developed on structural highs as salt flowed oceanward.

Karner and Gamboa (2007) have identified an unconformity at the salt – pre-salt contact across the entire Aptian salt basin, including the Santos, Campos and Espírito Santo basins in Brazil, and their conjugate basins in West Africa. The authors attribute the origin of this unconformity to be a lake level relative fall during the mid-late Aptian, triggered by a climate change. In the West African basins, the authors estimated at least 500 – 650 m of erosion measuring canyon cutting and incisions in early-mid Aptian clinoforms. Strugale and Catwright (2022) documented base-salt erosion in the hinge of fault-propagation folds, footwall blocks and one basement low in the northern Campos Basin. The authors interpreted the base-salt unconformity as a result of significant long-term sub-aerial exposure. Karner and Gamboa (2007) and Strugale and Cartwright (2022) also suggest that rift-related normal faults were locally active during salt deposition in the Santos and Campos basin, respectively, offsetting the base of the salt, and causing block uplift and erosion within basement lows.

Based on the above observations and in contrast to Alves et al. (2017), we argue that the base-salt unconformity formed *before* rather than after salt deposition. We suggest that the unconformity formed in response to base-level fall within a lacustrine environment (also stated by Karner and Gamboa, 2007), an interpretation supported by the presence of channel-like incision into the top of the pre-salt succession (e.g. Figure 10 b3). The unconformity is regional in extent due to the shallow bathymetry at that time, although the magnitude of incision may have been locally enhanced by local uplift around active faults, especially in the distal area.

Geodynamic models for the South Atlantic salt basins provide different potential explanations for the origin of this uplift. First, Karner and Gamboa (2007) suggest that heat advected during lithospheric thinning kept the middle - upper Aptian at relatively shallow depths. Second, Huismans and Beaumont (2011) propose that a widespread

shallow bathymetry requires an isostatic balance with sub-crustal emplacement of hot depleted lower-cratonic lithosphere, which is less dense than upwelled asthenosphere. Finally, Huismans and Beaumont (2014) use numerical models to demonstrate that counterflow of cratonic lithosphere can cause exposure of large regions of continental lithosphere in the outer region of a margin.

### 5.2. Seismic-stratigraphic expression of the syn- and post-rift stages of the Campos Basin

The lower pre-salt interval is characterised by divergent reflections within wedge-shaped packages syn-tectonic to rift-related normal faults (Figure 11). Such growth strata record fault activity, and, for that reason, are classified as syn-tectonic (Péron-Pinvidic et al., 2007) *and* syn-rift (Masini et al., 2013). The unconformity capping these strata record a time when rifting had migrated oceanward, but not to such an extent that all inboard faults were inactive in the distal area (see previous item; Figure 9).

The upper pre-salt interval is composed of subparallel and relatively continuous reflections typically contained within lenticular packages that thickens towards the centre of basement lows, but that are locally divergent (Figure 7b, between the Badejo High and the Corvina-Parati Low; Figure 9 – see numbered faults; Figure 11). This interval occurs within and above most of the rift-related depocentres, in contrast to that characterizing the underlying unit, which is typically localized within individual grabens. For that reason, the base of this succession contains reflections that onlap basement highs or the mid-pre-salt surface, indicating an increase in depositional area when compared to the underlying interval. Based on the age constraints most accepted in the literature (i.e., c. 123 – 116 Ma; Karner and Gamboa 2007; Winter et al., 2007), the pre-salt interval can

be classified as syn-rifting, given it is pre-breakup (c. 115 Ma, Heine et al., 2013). The aforementioned seismic-stratigraphic characteristics of the pre-salt interval indicate it is post-tectonic at a margin scale, although locally, it can also be syn-tectonic, i.e., faulted and/or exhibit thickening towards a few normal faults.

The origin of a late-rift sag-geometry basin characterised by limited upper crustal faulting and shallow water depths can be explained by depth-dependent extension (Karner and Gamboa, 2007; Huismans and Beaumont, 2011; Huismans and Beaumont, 2014). Karner and Gamboa (2007) suggest that depth-dependent extension during the late Aptian on the West African and Brazilian margins caused greater thinning of the lower crust and underlying lithosphere when compared to the upper crust. This mechanism generated sufficient accommodation for the deposition of the upper Aptian pre-salt sequence and the c. 2 km-thick evaporite sequence itself (Karner and Gamboa, 2007). Other possible depth-dependent mechanisms are sub-crustal emplacement of hot depleted lower-cratonic lithosphere (Huismans and Beaumont, 2011), or counterflow of cratonic lithosphere (Huismans and Beaumont, 2014).

Based on the age constraints most accepted in the literature for salt deposition, (110 – 116 Ma; Moreira et al., 2007; Gamboa et al., 2008; Szatmari et al., 2021), and for the continental breakup in southern Campos Basin (c. 115 Ma – Heine et al., 2013; Moulin et al., 2013), the salt could be syn- to post-rift, given it could be pre-, syn- or post-breakup. However, considering what is most accepted in works that address the South Atlantic evolution, salt deposition was synchronous in both West Africa and SE Brazil margins, being pre- to syn-breakup (e.g. Karner and Gamboa, 2007; Torsvik et al., 2009; Heine et al., 2013; Kukla et al., 2018; Pérez-Gussinyé, 2020; Szatmari et al., 2021). This means that the salt is syn-rifting.

We also show that the classical models of rift basins that use the geometry and seismic facies of the sedimentary units in order to classify distinct tectono-stratigraphic stages (e.g. Prosser, 1993; Bosence, 1998; Gawthorpe and Leeder, 2000) work well to describe the filling of individual half-grabens, but cannot be applied to rifted margins, such as Campos Basin. Due to the limited geophysical imaging available in the past, these models were based on the acquisition of data from one or only several adjacent basins exposed in the field or imaged in the subsurface (Peron-Pinvidic and Manatschal, 2019). Consequently, little was known about the structure and stratigraphy of the distal domains of rift systems. Improvements in seismic imaging, analytical methods, and computing capabilities, combined with deep sea drilling showed that the distal domains of rifted margins are different from the proximal ones, and new concepts and models emerged. Modern concepts now include polyphase (or multiphase) rifting, rift domain names (e.g. necking domain) and migration of deformation (e.g. Ranero and Pérez-Gussinyé, 2010; Brune et al., 2014; Pérez-Gussinyé et al., 2020; Chenin et al., 2021). This new terminology is still debated, and it is clear that terms such as syn-rift, post-rift, and breakup unconformity need to be revised (Masini et al., 2013).

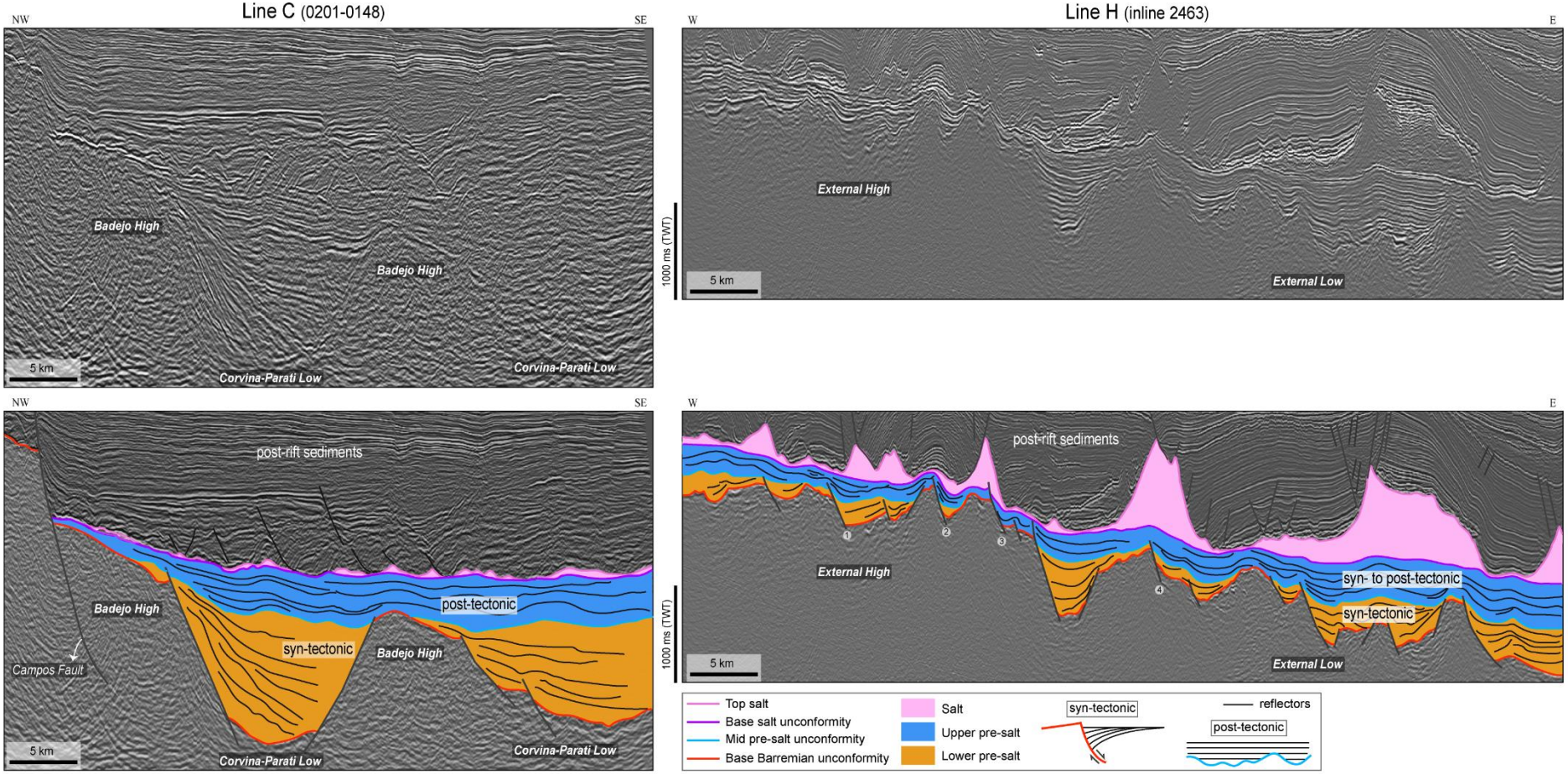


**Figure 11**. Uninterpreted and interpreted lines C and H, with the mapped stratigraphic surfaces and tectono-stratigraphic intervals. Some reflectors are traced in black to evidence syn-, post- and syn- to post-tectonic configurations (*sensu* Péron-Pinvidic et al., 2007). See Figure 3 for the location of the lines.

## 6. Conclusions

We use 2D and 3D seismic reflection and borehole data from the south-central Campos Basin to discuss the syn- to post-rift transition. The key conclusions of our study are:

1. We identified four key stratigraphic surfaces in the study area, which define three intervals with distinct geometries and seismic facies filling rift-related topography in Campos Basin: *lower pre-salt*, *upper pre-salt* and *salt*.
2. The lower pre-salt interval is characterised by divergent reflections interpreted as being syn-rift, syn-tectonic continental lake deposits, thickening towards graben and half-graben-bounding normal faults. This stage ends with the development of an angular unconformity (mid-Aptian or pre-neo-Alagoas) that records a time when rifting had migrated oceanward.
3. The upper pre-salt interval is typically defined of subparallel and relatively continuous reflections composing a broadly lenticular geometry that thickens towards the centre of basement lows, but that locally diverge towards rift-related normal faults, being characterised as syn-rifting and post-tectonic in the proximal area, and syn- to post-tectonic in the distal area. This unit is bounded on the top by an erosional unconformity identified on and adjacent to basement highs, which is inferred to have formed due to base-level fall and uplift associated with local fault reactivation.
4. The top-salt is a concordant surface with the overlying Albian carbonates.
5. The lower and upper pre-salt intervals are separated by a rift migration unconformity (*sensu* Pérez-Gussinyé et al., 2020) that predates and is not related to the breakup event.

## Acknowledgments

F.B. Amarante thanks CNPq (National Council for Scientific and Technological Development of Brazil) for the doctorate scholarship. We thank Mohamed Gouiza, Michael Strugale and the anonymous reviewer for their constructive insights, and the associate editor Cari Johnson for her editorial handling. The authors gratefully acknowledge ANP (Brazil's National Oil, Natural Gas and Biofuels Agency) for providing the data and for the license to publish this article.

## References

Abrahão, D., Warme, J.E., 1990. Lacustrine and associated deposits in a rifted continental margin e lower cretaceous Lagoa Feia formation, Campos Basin, offshore Brazil. In: Katz, B.J. (Eds.), Lacustrine Basin Exploration: Case Studies and Modern Analogs. AAPG 50, 287–305.

Allen, P.A., Allen, J.R. 2005. Basin analysis: principles and applications. (second ed.), Wiley-Blackwell Publishing, Sydney, p. 560

Alvarenga, R.d.S., Kuchle, J., Iacopini, D., Goldberg, K., Scherer, C.M.d.S., Pantopoulos, G., Ene, P.L., 2021. Tectonic and Stratigraphic Evolution Based on Seismic Sequence Stratigraphy: Central Rift Section of the Campos Basin, Offshore Brazil. Geosciences 11, 338. https://doi.org/10.3390/geosciences11080338

Alves, T.M., Fetter, M., Lima, C., Cartwright, J.A., Cosgrove, J., Gangá, A., Queiroz, C.L., Strugale, M., 2017. An incomplete correlation between pre-salt topography, top reservoir erosion, and salt deformation in deep-water Santos Basin (SE Brazil). Marine and Petroleum Geology 79, 300–320. https://doi.org/10.1016/j.marpetgeo.2016.10.015

Amarante, F.B., Jackson, C.A., Pichel, L.M., Scherer, C.M.S., Kuchle, J., 2021. Pre-salt rift morphology controls salt tectonics in the Campos Basin, offshore SE Brazil. Basin Research 33 (5), 2837–2861. https://doi.org/10.1111/bre.12588

Amarante, F.B., Kuchle, J., Iacopini, D., Scherer, C.M.S., Alvarenga, R.S., Ene, P.L., Schilling, A.B., 2020. Seismic tectono-stratigraphic analysis of the Aptian pre-salt marginal system of Espírito Santo Basin, Brazil. Journal of South American Earth Sciences 98, 102474. https://doi.org/10.1016/j.jsames.2019.102474

Araujo, M.N., Pérez-Gussinyé, M., Muldashev, I., 2022. Oceanward rift migration during formation of Santos–Benguela ultra-wide rifted margins. Geological Society London Special Publications 524 (1), SP524-2021-123. https://doi.org/10.1144/sp524-2021-123

Beglinger, S.E., Doust, H., Cloetingh, S., 2012. Relating petroleum system and play development to basin evolution: West African South Atlantic basins. Marine and Petroleum Geology 3, 1–25.

Bosence, D.W.J., 1998. Stratigraphic and sedimentological models of rift basins. In: Purser, B.H., Bosence, D.W.J. (Eds.), Sedimentation and Tectonics of Rift Basins: Red Sea, Gulf of Aden. London: Chapman e Hall. 9–25.

Bott, M.P.H., 1995. Rifted passive margins. In: Olsen, K.H. (Eds.) Continental Rifts: Evolution, Structure, Tectonics. Developments in Geotectonics 25, 409–426

Braun, J., Beaumont, C., 1989. A physical explanation of the relation between flank uplifts and the breakup unconformity at rifted continental margins. Geology 17, 760–764.

Bruhn, C.H.L., Gomes, J.A.T., Del Lucchese, C., Jr., Johann, P.R.S., 2003. Campos Basin: Reservoir Characterization and Management - Historical Overview and Future Challenges, in: Offshore Technology Conference. Presented at the Offshore Technology Conference, Offshore Technology Conference. https://doi.org/10.4043/15220-ms

Brune, S., Heine, C., Pérez-Gussinyé, M., Sobolev, S.V., 2014. Rift migration explains continental margin asymmetry and crustal hyper-extension. Nature Communications 5, 4014.

Cainelli, C., Mohriak, W.U., 1999. Some remarks on the evolution of sedimentary basins along the eastern Brazilian continental margin. Episodes, 22 (3), 206–216.

Cartwright, J., 1991. The kinematic evolution of the Coffee Soil Fault. Geological Society, London, Special Publications 56, 29–40.

Chang, H.K., Kowsmann, R.O., Figueiredo, A.M.F., Bender, A., 1992. Tectonics and stratigraphy of the East Brazil rift system: an overview. Tectonophysics 213, 97–138.

Chenin, P., Manatschal, G., Ghienne, J., Chao, P., 2021. The syn-rift tectono-stratigraphic record of rifted margins (Part II): A new model to break through the proximal/distal interpretation frontier. Basin Research 00, 1–44. https://doi.org/10.1111/bre.12628

Chenin, P., Manatschal, G., Lavier, L.L., Erratt, D., 2015. Assessing the impact of orogenic inheritance on the architecture, timing and magmatic budget of the North Atlantic rift system: A mapping approach. Journal of the Geological Society of London, 172, 711–720. https://doi.org/10.1144/jgs20 14-139

Davison, I., 2007. Geology and tectonics of the South Atlantic Brazilian salt basins. Geological Society, London, Special Publications 272, 345–359. https://doi.org/10.1144/gsl.sp.2007.272.01.18

Davison, I., Anderson, L., Nuttall, P., 2012. Salt deposition, loading and gravity drainage in the Campos and Santos salt basins. Geological Society, London, Special Publications 363, 159–174. https://doi.org/10.1144/sp363.8

Dias, J.L., Oliveira, J.Q., Vieira, J.C., 1988. Sedimentological and stratigraphyc analysis of the Lagoa Feia Formation, rift phase of Campos Basin, offshore Brazil. Revista Brasileira de Geociências 18 (3), 252–260.

Dooley, T.P., Hudec, M.R., Carruthers, D., Jackson, M.P.A., Luo, G., 2017. The effects of base-salt relief on salt flow and suprasalt deformation patterns — Part 1: Flow across simple steps in the base of salt. Interpretation 5, SD1–SD23. https://doi.org/10.1190/int-2016-0087.1

Falvey, D., 1974. The development of continental margins in plate tectonic theory. J. Aust. Pet. Explor. Assoc. 14, 95–106.

Fetter, M., 2009. The role of basement tectonic reactivation on the structural evolution of Campos Basin, offshore Brazil: Evidence from 3D seismic analysis and section restoration. Marine and Petroleum Geology 26, 873–886. https://doi.org/10.1016/j.marpetgeo.2008.06.005

Freitas, R.T.J., 2006. Ciclos deposicionais evaporiticos da bacia de Santos: una analise cicloestratigrafica a partir de dados de 2 poços e de traços de sísmica. Masters thesis, Instituto de Geociencias, Universidade Federal do Rio Grande do Sul, Brazil.

Gamboa, L.A.P., Machado, M.A.P., Silviera, D.P., Freitas, J.T.R., Silva, S.R.P., 2008. Evaporitos estratificados no Atlântico Sul: interpretação sísmica e controle tectono-estratigráfico na Bacia de Santos. In: Mohriak, W., Szatmari, P., Anjos, S.M.C. (Eds.) Sal: Geologia e Tectonica. Editora Beca, São Paulo, Brazil, 340–359.

Gawthorpe, R.L., Leeder, M.R., 2000. Tectono-sedimentary evolution of active extensional basins. Basin Research 12, 195–218.

Goldberg, K., Kuchle, J., Scherer, C.M.S., Alvarenga, R.S., Ene, P.L., Armelenti, G., De Ros, L.F., 2017. Re-Sedimented deposits in the rift section of the Campos Basin. Marine and Petroleum Geology 80, 412–431.

Guardado, L.R., Gamboa, L.A.P., Lucchesi, C.F., 1989. Petroleum geology of Campos Basin, Brazil: a model for producing Atlantic type basin. In: Edwards, J.D., Santagrossi, P.A. (Eds.), Divergent/Passive Margins Basins. AAPG Memoir 48, 3–36.

Guardado, L.R., Spadini, A.R., Brandão, J.S.L., Mello, M.R., 2000. Petroleum system of the Campos Basin, Brazil. In: Mello, M.R., Katz, B.J. (Eds.), Petroleum Systems of South Atlantic Margins. AAPG Memoir 73, 317–324.

Heine, C., Zoethout, J., Müller, R. D., 2013. Kinematics of the South Atlantic rift. Solid Earth, 4(2), 215–253. https://doi.org/10.5194/se-4-215-2013

Hiscott, R.N., Wilson, R.C.L., Gradstein, F.M., Pujalte, V., Garcia-Mondejar, J., Boudreau, R.R.D. Wishart, H.A., 1990. Comparative stratigraphy and subsidence history of Mesozoic rift basins of North Atlantic. American Association of Petroleum Geologists Bulletin 74, 60–76.

Huismans, R.S., Beaumont, C., 2014. Rifted continental margins: The case for depth-dependent extension. Earth and Planetary Science Letters 407, 148–162.
https://doi.org/10.1016/j.epsl.2014.09.032

Huismans, R.S., Beaumont, C., 2011. Depth-dependent extension, two-stage breakup and cratonic underplating at rifted margins. Nature 473, 74–78. http://dx.doi.org/10.1038/nature09988

Issler, D., McQueen, H., Beaumont, C. 1989. Thermal and isostatic consequences of simple shear extension of the continental lithosphere. Earth and Planetary Science Letters 91, 341–358.

Jagoutz, O., Müntener, O., Manatschal, G., Rubatto, D., Péron-Pinvidic, G., Turrin, B.D., Villa, I.M., 2007. The rift-to-drift transition in the North Atlantic: A stuttering start of the MORB machine? Geology, 35, 1087–1090.

Jackson, M.P.A., Cramez, C. & Fonck, J-M., 2000. Role of subaerial volcanic rocks and mantle plumes in creation of South Atlantic margins: implications for salt tectonics and source rocks, Marine and Petroleum Geology 17, 477–498.

Karner, G.D., Gamboa, L.A.P., 2007. Timing and origin of the South Atlantic pre-salt sag basins and their capping evaporates. In: Schreiber, B.C., Lugli, S., Babel, M. (Eds.) Evaporites through Space and Time. Geological Society, London, Special Publications 285, 15–35.

Kuchle, J., Scherer, C.M.S., 2010. Sismoestratigrafia de bacias rifte: técnicas, métodos e sua aplicação na Bacia do Recôncavo. Boletim de Ciências da Petrobrás 18 (2), 179–206.

Kukla, P.A., Strozyk, F., Mohriak, W.U., 2018. South Atlantic salt basins – Witnesses of complex passive margin evolution. Gondwana Research 53, 41–57. https://doi.org/10.1016/j.gr.2017.03.012

Lima, B.E.M., De Ros, L.F., 2019. Deposition, diagenetic and hydrothermal processes in the Aptian Pre-Salt lacustrine carbonate reservoirs of the northern Campos Basin, offshore Brazil. Sedimentary Geology 383, 55–81. https://doi.org/10.1016/j.sedgeo.2019.01.006

Manatschal, G., Chenin, P., Ghienne, J.-F., Ribes, C., Masini, E., 2022. The syn-rift tectono-stratigraphic record of rifted margins (Part I): Insights from the Alpine Tethys. Basin Research 34, 457– 488. https://doi.org/10.1111/bre.12627

Masini, E., Manatschal, G., Mohn, G., 2013. The Alpine Tethys rifted margins: Reconciling old and new ideas to understand the stratigraphic architecture of magma-poor rifted margins. Sedimentology 60, 174–196. https://doi.org/10.1111/sed.12017

Mizusaki, A.M.P., Petrini, R., Bellieni, Comin-Chiaramonti, P., Dias, J., De Min, A., Piccirillo., E.M. 1992. Basalt magmatism along the passive continental margin of SE Brazil (Campos basin). Contributions to Mineralogy and Petrology 111, 143–160. https://doi.org/10.1007/BF00348948

Mohn, G., Manatschal, G., Müntener, O., Beltrando, M., Masini, E., 2010. Unravelling the interaction between tectonic and sedimentary processes during lithospheric thinning in the Alpine Tethys margins. International Journal of Earth Sciences 99, 75–101.

Mohriak, W., Nemčok, M., Enciso, G., 2008. South Atlantic divergent margin evolution: rift-border uplift and salt tectonics in the basins of SE Brazil. Geological Society, London, Special Publications 294, 365–398. https://doi.org/10.1144/sp294.19

Moreira, J.L.P., Madeira, C.V., Gil, J.A., Machado, M.A.P., 2007. Bacia de Santos. Boletim da Geociências da Petrobras, Rio de Janeiro, 15, 531–549.

Morley, C.K., 2002. Evolution of large normal faults: Evidence from sesmic refletion data. AAPG Bulletin 86 (6), 961–978.

Moulin, M., Aslanian, D., Unternehr, P., 2010. A new starting point for the South and Equatorial Atlantic Ocean. Earth-Science Reviews 98, 1–37.

Moulin, M., Aslanian, D., Rabineau, M., Patriat, M., Matias, L., 2013. Kinematic keys of the Santos–Namibe basins. Geological Society, London, Special Publications 369, 91–107. https://doi.org/10.1144/sp369.3

Nottvedt, A., Gabrielsen, R.H., Steel, R.J., 1995. Tectonostratigraphy and sedimentary architecture of rift basins, with reference to the northern North Sea. Marine and Petroleum Geology 12 (8), 881–901. https://doi.org/10.1016/0264-8172(95)98853-w

Pérez-Gussinyé, M., Andrés-Martínez, M., Araújo, M., Xin, Y., Armitage, J., & Morgan, J. P., 2020. Lithospheric strength and rift migration controls on synrift stratigraphy and breakup unconformities at rifted margins: Examples from numerical models, the Atlantic and South China Sea margins. Tectonics, 39, e2020TC006255. https://doi.org/10.1029/2020TC006255

Péron-Pinvidic, G., Manatschal, G., Minshull, T.A., Sawyer, D.S., 2007. Tectonosedimentary evolution of the deep Iberia-Newfoundland margins: Evidence for a complex breakup history. Tectonics 26(2), TC2011.

Péron-Pinvidic, G., Manatschal, G., 2009. The final rifting evolution at deep magma-poor passive margins from Iberia–Newfoundland: a new point of view. International Journal of Earth Sciences 98, 1581–1597.

Péron-Pinvidic, G., Manatschal, G., Osmundsen, P.T., 2013. Structural comparison of archetypal Atlantic rifted margins: A review of observations and concepts. Marine and Petroleum Geology 43, 21–47. https://doi.org/10.1016/j.marpetgeo.2013.02.002

Peron-Pinvidic, G., Manatschal, G., 2019. Rifted Margins: State of the Art and Future Challenges. Frontiers in Earth Sciences 7:218. https://doi.org/10.3389/feart.2019.00218

Prosser, S., 1993. Rift-related linked depositional systems and their seismic expression. In: Williams, G.D., Dobb, A. (Eds.), Tectonics and Seismic Sequence Stratigraphy. Geological Society of London, London, Special Publication 71, 35–66.

Quirk, D.G., Hertle, M., Jeppesen, J.W., Raven, M., Mohriak, W.U., Kann, D.J., Nørgaard, M., Howe, M.J., Hsu, D., Coffey, B., Mendes, M.P., 2013. Rifting, subsidence and continental break-up above a mantle plume in the central South Atlantic. Geological Society, London, Special Publications 369, 185–214. https://doi.org/10.1144/sp369.20

Ranero, C.R., Pérez-Gussinyé, M., 2010. Sequential faulting explains the asymmetry and extension discrepancy of conjugate margins. Nature 468, 294–299. https://doi.org/10.1038/nature09520

Rangel, H.D., Martins, F.A.L., Esteves, F.R., Feijó, F.J., 1994. Bacia de Campos. Boletim de Geociências da Petrobras 8 (1), 203–218.

Roberts, A.M., Yielding, G., 1991. Deformation around basin-margin faults in the North Sea/mid-Norway rift. Geological Society, London, Special Publications 56, 61–78. https://doi.org/10.1144/gsl.sp.1991.056.01.05

Rowan, M.G., Peel, F.J., Vendeville B.C., 2004, Gravity-driven fold belts on passive margins. In McClay, K.K. (Eds.), Thrust tectonics and hydrocarbon systems: AAPG Memoir 82, 157–182.

Sibuet, J.C., Srivastava, S., Manatschal, G., 2007. Exhumed mantle-forming transitional crust in the Newfoundland-Iberia rift and associated magnetic anomalies. Journal of Geophysical Research 112, B06105.

Stokes, W.L., 1982. Essentials of Earth History 4th Edition. Prentice Hall Inc, 65 p. ISBN 0-13-285890-8

Strugale, M., Cartwright, J., 2022. Tectono-stratigraphic evolution of the rift and post-rift systems in the Northern Campos Basin, offshore Brazil. Basin Research 00, 1–33. https://doi.org/10.1111/bre.12674

Szatmari, P., 2000. Habitat of petroleum along the South Atlantic margins. In: Mello, M.R., Katz, B.J. (Eds.), Petroleum Systems of South Atlantic Margins: AAPG Memoir 73, 69–75.

Szatmari, P., de Lima, C. M., Fontaneta, G., de Melo Lima, N., Zambonato, E., Menezes, M. R., Bahniuk, J., Coelho, S. L., Figueiredo, M., Florencio, C. P., 2021. Petrography, geochemistry and origin of South Atlantic evaporites: The Brazilian side. Marine and Petroleum Geology, 127, 104805. https://doi.org/10.1016/j.marpe tgeo.2020.104805

Tedeschi, L. R., Jenkyns, H. C., Robinson, S. A., Lana, C. C., Menezes Santos, M. R. F., Tognoli, F. M. W., 2019. Aptian carbon-isotope record from the Sergipe-Alagoas Basin: New insights into oceanic anoxic event 1a and the timing of seawater entry into the South Atlantic. Newsletters on Stratigraphy, 53, 529. https://doi.org/10.1127/nos/2019/0529

Torsvik, T.H., Rousse, S., Labails, C., Smethurst, M.A., 2009. A new scheme for the opening of the South Atlantic Ocean and the dissection of an Aptian salt basin. Geophysical Journal International 177, 1315–1333.

Weijermars, R., Jackson, M.P.A., Dooley, T.P., 2014. Quantifying drag on wellbore casings in moving salt sheets. Geophysical Journal International 198, 965–977.

Winter, W.R., Jahnert, R.J., França, A.B., 2007. Bacia de Campos. Boletim de Geociências da Petrobras 15(2), 511–529.